

# RCU2 testing and design

***Inge Nikolai Torsvik***



*Master Thesis*

*Department of Physics and Technology  
University of Bergen*

*June 2014*

## **Abstract**

# **Contents**

# Contents

<b>1</b>	<b>Introduction</b>	<b>1</b>
1.1	How to test . . . . .	2
1.2	About this work . . . . .	2
<b>2</b>	<b>ALICE experiment</b>	<b>4</b>
2.1	The Time Projection Chamber TPC . . . . .	6
2.2	The TPC Front End electronics FEE . . . . .	6
2.2.1	Front End Card FEC . . . . .	7
2.2.2	Readout Control Unit RCU . . . . .	8
2.2.3	RCU2 . . . . .	8
<b>3</b>	<b>Radiation and Radiation effect on Semiconductor devices</b>	<b>11</b>
3.1	Interaction of Radiation With Matter . . . . .	11
3.2	Charge particle and their Interaction with Matters . . . . .	12
3.2.1	Stopping Power . . . . .	12
3.2.2	Specific Stopping Power . . . . .	13
3.2.3	Linear Energy Transfer LET . . . . .	14

3.3	Neutral particle and their Interaction with Matter . . . . .	15
3.3.1	Neutrons . . . . .	15
3.3.2	Photons . . . . .	15
3.4	Radiation Effects on Semiconductor Devices . . . . .	15
3.4.1	Single Events Effects SEE . . . . .	16
3.4.2	Accumulative Effects . . . . .	18
3.4.3	The TPC radiation environment . . . . .	19
<b>4</b>	<b>Preparations for Testing</b>	<b>21</b>
4.1	The Integrated Circuits (ICs) . . . . .	21
4.1.1	TPS51200 . . . . .	22
4.1.2	MIC69302WU . . . . .	23
4.1.3	SN74AVCB164245 . . . . .	23
4.1.4	SN74AVC2T245 . . . . .	24
4.1.5	QS3VH257 . . . . .	25
4.1.6	SY89831U . . . . .	26
4.1.7	ADN2814 and MAX3748 . . . . .	27
4.1.8	INA210 . . . . .	29
4.1.9	TLV3011 . . . . .	29
4.1.10	All the test boards . . . . .	30
4.2	Software . . . . .	32
4.3	SmartFusion2 . . . . .	32

4.3.1	SRAM test . . . . .	33
4.3.2	Test of the Logical element . . . . .	34
4.3.3	Single Event Latchup and PLL . . . . .	35
4.3.4	Configuration and Monitoring . . . . .	36
4.4	Equipment used for testing . . . . .	37
4.4.1	SRAM detector . . . . .	38
4.4.2	Scintillator counter . . . . .	39
4.4.3	X-Y-positioning system . . . . .	40
<b>5</b>	<b>Irradiation test setup</b>	<b>41</b>
5.1	Irradiation on Oslo Cyclotron Laboratory (OCL) . . . . .	41
5.1.1	About OCL . . . . .	41
5.1.2	Experiment setup and equipment . . . . .	42
5.1.3	Preparation and characterization of the beam . . . . .	43
5.1.4	What was tested at OCL . . . . .	46
5.2	Testing at The Svedberg Laboratory (TSL) . . . . .	47
5.2.1	About TSL . . . . .	47
5.2.2	Beam setup procedure . . . . .	47
5.2.3	What was tested at TSL . . . . .	48
<b>6</b>	<b>Calculations and Results from Beam Test</b>	<b>49</b>
6.1	Calculation of dose . . . . .	49

6.1.1	Definitions . . . . .	50
6.1.2	Calculating dose using LET . . . . .	50
6.1.3	Calculating dose using FLUKA simulations . . . . .	52
6.1.4	Comparison of LET and FLUKA . . . . .	53
6.2	Results from OCL . . . . .	55
6.2.1	Calibration process . . . . .	55
6.2.2	Test results . . . . .	57
6.2.3	TPS51200 . . . . .	60
6.2.4	MIC69302WU . . . . .	60
6.2.5	SN74AVCB164245 . . . . .	61
6.2.6	SN74AVC2T245 . . . . .	61
6.2.7	QS3VH257 . . . . .	62
6.2.8	SY89831 . . . . .	63
6.2.9	ADN2814 . . . . .	63
6.2.10	MAX3748 . . . . .	65
6.3	Discussion of the result . . . . .	66
<b>7</b>	<b>Conclusion</b>	<b>67</b>
<b>Appendix A</b>	<b>Some Appendix</b>	<b>68</b>
A.1	Beam setup data . . . . .	68

<b>CERN</b>	European Council for Nuclear Research
<b>ALICE</b>	A Large Ion Collider Experiment
<b>OCL</b>	Oslo Cyclotron Laboratory
<b>DUT</b>	Device Under Test
<b>RCU</b>	Readout Control Unit
<b>LHC</b>	Large Hadron Collider
<b>FEE</b>	Front End Electronic
<b>FEC</b>	Front End Card
<b>FPGA</b>	Field Programmable Gate Array
<b>SEE</b>	Single Even Effect
<b>SEU</b>	Single Event Upset
<b>SET</b>	Single Event Transient
<b>SEL</b>	Single Event Latchup
<b>IC</b>	Integrated Circuit
<b>PCB</b>	Printed Circuit Board
<b>LVDS</b>	Low-Voltage Differential Signaling
<b>DAQ</b>	Data Acquisition
<b>SF2</b>	SmartFusion2
<b>CML</b>	Current-Mode Logic
<b>TPC</b>	Time Projection Chamber
<b>LVPECL</b>	Low Voltage Positive Emitter Coupled Logic
<b>SRAM</b>	Static Random Access Memory
<b>TID</b>	Total Ionizing Dose
<b>UART</b>	Universal Asynchronous Receiver/Transmitter
<b>ADC</b>	Analog to Digital Converter
<b>LET</b>	Linear Energy Transfer
<b>SoC</b>	System On a Chip
<b>CMOS</b>	Complementary Metal Oxide Semiconductor

<b>DCS</b>	Control System board
<b>SIU</b>	Source Interface Unit
<b>TSL</b>	The Svedberg Laboratory
<b>MSS</b>	Microcontroller SubSystem
<b>WSR</b>	Windowed Shift Register

# Chapter 1

## Introduction

At CERN (European Council for Nuclear Research) in Switzerland there are being conducted experiment on fundamental structure of the universe. This is done by accelerating particles up to a energy of 4 TeV per proton, and then collide with other particles on the same energy level. The largest accelerator is called Large Hadron Collider (LHC), and is the largest particle accelerator ever built, installed in a 27 km long tunnel. Particles are accelerated in both direction in the LHC. When the particles has reached high enough energy, particles from opposite direction are made to crash at 4 experiment areas, one of these is called ALICE (A Large Ion Collider Experiment). A Large Ion Collider Experiment (ALICE) is built to study a matter known as Quark-gluons plasma [1], which will be generated under collisions of heavy ions. ALICE consist of several sub-detector with different functionality. Time Projection Chamber (TPC) is one of these, and is the main tracking detector placed closes to the beam-line, see section 2. Under a collision high particles will be generated, and will also pose a risk to the electronics used. It is therefore of highest importance to test everything that are planed to be used in the experiment for radiation.

One of the main boards used in the TPC detector is the Readout Control Unit (RCU). Now there has been decided that a new RCU shall be made, namely the RCU2. Because of the radiation level in the LHC, every active component used in the design of the RCU2 has to be tested for radiation to be sure that it won't fail when it is installed in the TPC detector.

## 1.1 How to test

The radiation tests done through this work is mainly test for accumulative effects. Accumulative effects are effects caused by the total radiation of a component, and are measured by the functionality and power consumption of the component, see section 3.4.2 for more information.

Previous research has been done on the radiation level in ALICE [2] and [15], and are used to decide if the tested components can be used or not.

Test for Single Event Effects (SEEs) like Single Event Upset (SEU), Single Event Transient (SET) and Single Event Latchup (SEL) on a Microsemi SmartFusion2 (SF2) System On a Chip (SoC) Field Programmable Gate Array (FPGA) have also been performed.

## 1.2 About this work

I started working on the RCU2-project in the autumn of 2013. Already before I started working, the design and the schematic layout for the RCU2 was basically finished. In the design process components that was already tested or are proven to be radiation hard was used when possible, but such components weren't always available. So my work in the project has been to do irradiation tests on components for the RCU2 design which didn't have any record of being radiation tested before.

The ICs which I have tested consist of: SoC FPGA, power regulators, bus transceivers, limiting amplifier, multiplexer/demultiplexer, buffer, comparator and Current Shunt Monitor. In order to investigate the radiation tolerance of these circuits, I had to first acquire good knowledge of radiation induced effect that may occur in such devices. I also needed to study these components to be able to find a reasonable test methodology. Further, I had to familiarize myself with CAD tools such as *expedition PCB* and *DXdesigner* and programming and developing environments like Libero and labVIEW in order to develop a sufficient hardware and software based test setup for the components.

The RCU2's main FPGA the microsemi SF2, has been the main focus through this work. That is because this component will be hard to replace, and a functional failure on this one, may set the whole RCU2 out of function. The radiation effects that was tested on for SF2 are, SRAM blocks for SEU, logic elements for SEU and SET, and in general SEL. These effects can be read about in section 3.4.1.

The irradiation test was executed in four periods, three times at OCL with a

proton beam of 28 MeV and 25 MeV where all components have been tested, and one time at TSL with a proton beam of 180 MeV, where only the SF2 SoC FPGA was tested. A SF2 starter-kit was used when designing test for this IC, and test code was written in VHDL and C. To be able to detect SEL the current on the FPGA had to be measured. Therefore a current measurement board was made for that task.

To summarize, this work has been consisting of practical work like making Printed Circuit Boards (PCBs), writing test code in VHDL, making labVIEW programs and making test codes in C. It has also consisting on getting the necessary knowledge of the components tested, learning to program in VHDL and C, as well as learning to use the tools and programs for the different tasks.

# Chapter 2

## ALICE experiment

Since 1954 physicists at European Council for Nuclear Research (CERN) have studied the nucleus and its structure to find the fundamental structure of the universe. CERN is the world largest research center for nuclear and particle physics, and has a total of 21 member state. One of the biggest attraction at CERN is the Large Hadron Collider (LHC), that is a circular particle accelerator placed in a 27 km long tunnel around 100 meter beneath ground level. This is the last accelerator in a chain of up to 7 (depending on which particle to accelerate), see picture 2.0.1, where the particles gradually accelerate to higher and higher energies, up to their maximum energy of 4 TeV and speed close to the speed of light. When particles has reached this energy level accelerated particles from opposite direction are made to collide inside 4 different experiment areas, where one of these is called A Large Ion Collider Experiment (ALICE), see figure 2.0.2.

The ALICE detector is a heavy ion detector. Its main purpose is to study a state of matter called quark-gluon plasma which will be generated when heavy ions collides. Under the collisions a temperature 100 000 times higher than the temperature of the sun is generated. There is then high enough energy to split the protons and neutrons, and achieve a plasma of unbound quarks and gluons, and that is called quark-gluon plasma.

All ordinary matter in today's universe is made up of atoms. Each atom contains a nucleus composed of protons and neutrons (except hydrogen, which has no neutrons), surrounded by a cloud of electrons. Protons and neutrons are in turn made of quarks bound together by other particles called gluons. No quark has ever been observed in isolation: the quarks, as well as the gluons, seem to be bound permanently together and confined inside composite particles, such as protons and neutrons.

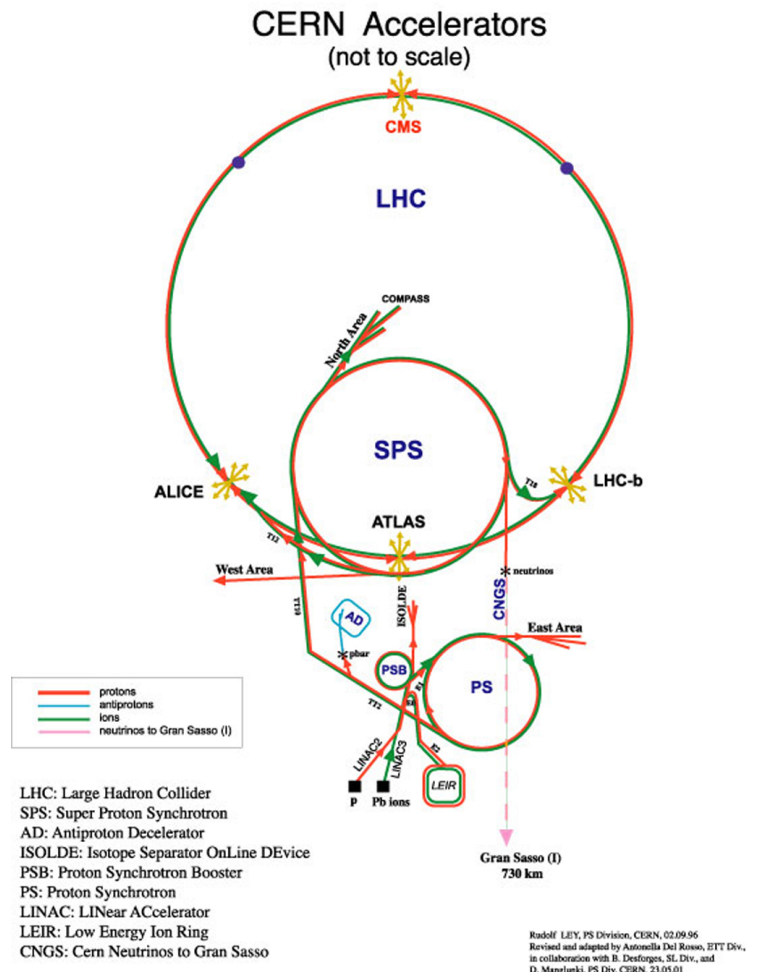


Figure 2.0.1: CERN accelerators [3]

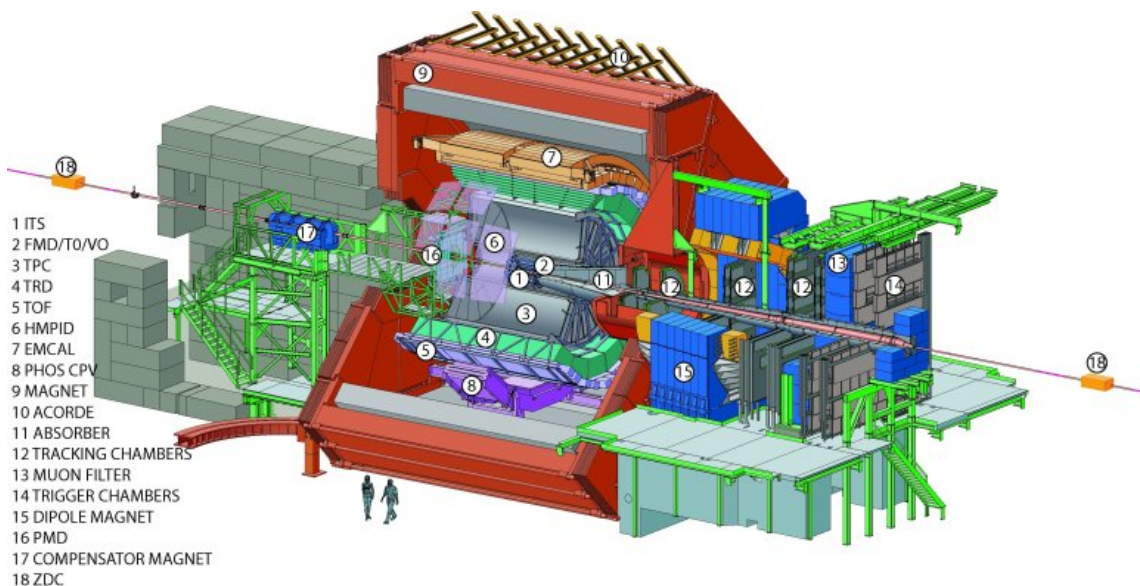


Figure 2.0.2: Layout of the ALICE experiment [4]

## 2.1 The Time Projection Chamber TPC

The ALICE detector comprises several sub-detectors, where one of these is the Time Projection Chamber (TPC). The TPC is the main tracking detector of ALICE. The function of TPC are tracking particles, measure the charged particles momentum and identification of particles. A drawing of the TPC can be seen in figure 2.1.1. The TPC detector has a cylindrical shape, with a inner radius of 85 cm and outer radius of 250 cm, and has an overall length of 510 cm. The detector is made up of a large cylindrical field cage, filled with  $88 \text{ m}^3$  of 90% Ne gas and 10%  $\text{CO}_2$  gas. A high voltage electrode is placed in the center of the detector, dividing the TPC into two drift regions, and making a electric field between electrode and the two end plates. When a charged particle is generated inside the detector, the gas inside the cage will be ionized. The free electrons and the ions will then drift in the electric field between the high voltage electrode and the two end plates. At the end-plates we find the Readout Chamber which are divided into 18 trapezoidal sectors, where each sector is again divided into the inner and outer chamber. In the readout chamber, there are a total of 560 000 readout pads.

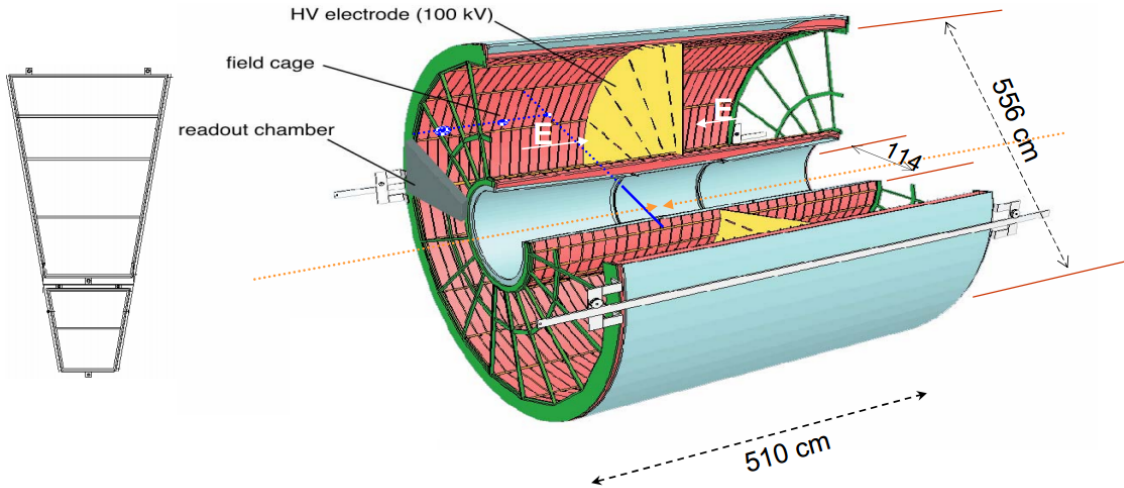


Figure 2.1.1: Layout of the TPC [4]

## 2.2 The TPC Front End electronics FEE

Each of the 36 sections ( $2 \times 18$ ) are also divided into 6 readout partitions, that is 2 in the inner chamber and 4 in the outer chamber. There are a total of 216 RCU connected to a total of 4356 Front End Card (FEC) which is connected to all of the 560 000 readout pads, and all together this sums up the Front End Electronic (FEE), see figure 2.2.1. In short, the task of the FEE is to read out the charge received at the readout pads, process it and send useful data to a computer.

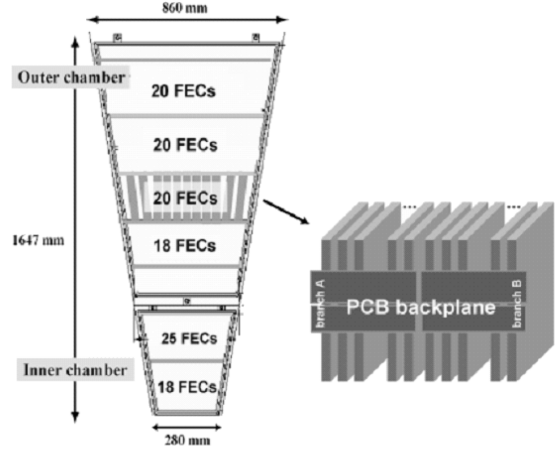


Figure 2.2.1: A TPC sector. Showing how FEC is placed [5]

### 2.2.1 Front End Card FEC

A current signal given by one of the pads, is sent into a Front End Card (FEC) which consist of three basic functional units, see block diagram in figure 2.2.2. The first unit is a charge sensitive amplifier/shaper called PASA, the second unit is a 10-bit 10 MHz low-power Analog to Digital Converter (ADC). The last unit is a digital circuit that perform the baseline subtraction, tail cancellation, zero-suppression<sup>1</sup>, formatting and buffering. The ADC and the digital unit together constitute the so called ALTRO chip. There are 16 PASA chips and 16 ALTRO chips on the FEC, the PASA chip is connected to 16 readout pads each, which gives a total of 128 readout pads for each FEC.

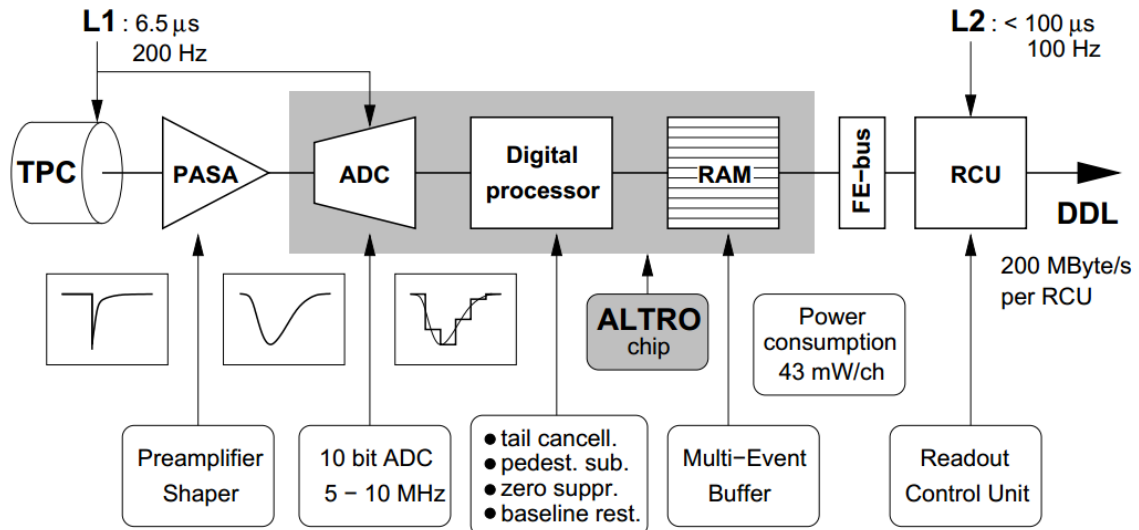


Figure 2.2.2: Block diagram of the Front End Card [4]

---

<sup>1</sup>Zero Compressions means that signal bellow a given threshold will be filtered away.

## 2.2.2 Readout Control Unit RCU

One Readout Control Unit (RCU) is connected to one row of FECs (up to 25 pieces), through a backplane<sup>2</sup>, see figure 2.2.1. The RCU task is to control all of the Front End Electronic (FEE) all the way from the readout pads through the FECs, and out to a Data Acquisition (DAQ) System. The RCU consist of three separated boards which are the Motherboard board, the Control System board (DCS) board and the Source Interface Unit (SIU) board. Most of the RCU functions is controlled by the Xilinx Virtex-II Pro FPGA. This FPGA are controlling the readout process of the TPC detector. It is also responsible for moving data from the FECs to the Source Interface Unit (SIU) board, where data is transmitted via a optical link to the Data Acquisition system, where data is stored and is made accessible for analysis.

The Xilinx Virtex-II Pro is a Static Random Access Memory (SRAM) based FPGA. SRAM cells are vulnerable for Single Event Upsets (SEUs), see section 3.4.1. Therefore a flash based FPGA, Actel ProASIC is used to monitor the SRAM memory and reprogram/reconfigure if an error occurs.

The DCS board is basically an embedded computer running Linux. This board is connected through a Ethernet link to a computer on the outside of the ALICE detector. Through it, we are even able to upgrade and reprogram the FPGAs of the RCU. So even though the hardware is inaccessible after it has been mounted in the TPC, the SIUs boards gives some kind of flexibility. In addition, it has an optical interface, receiving the clock and trigger information from the Timing, Trigger and Control system, also called TTC.

## 2.2.3 RCU2

### Why upgrade RCU

LHC is currently shut down for maintenance and preparation for even higher energies. This period, called Long Shutdown 1 (LS1), lasts until end of 2014. The present TPC readout electronics will be a limiting factor with the foreseen readout rate for the next run period (run2). The bus between RCU and FECs is not able to read all data for high occupancy events, like Pb-Pb collisions. In addition stability issues related to SEU on the SRAM based FPGA have been observed with the present setup. 9 % of the run time had to be stopped because of errors in the TPC readout electronics.

---

<sup>2</sup>A backplane is a PCB board, that connects Front End Cards to a Readout Control Unit. This is used instead of cables to get a more stability, and to keep things in place.

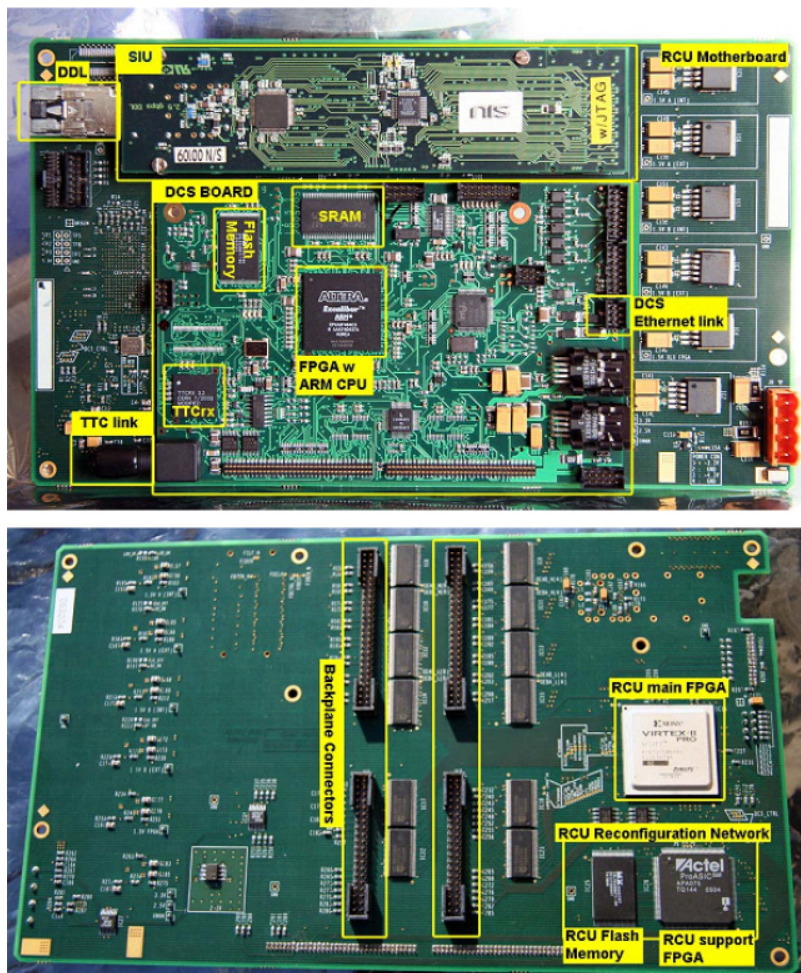


Figure 2.2.3: The Readout Control Unit top side and bottom side [5]

## The new Readout Control Unit, the RCU2

The main challenge with making the RCU2 was to develop a solution that gives the needed performance improvement, and at the same time was feasible within the limited time-frame. Therefore some of the old infrastructure has to be reused, like cables for Ethernet, Trigger and power and the cooling envelops.

The main difference between the RCU2 and RCU1 is that the main FPGA, the Xilinx Virtex-II Pro, has been replaced by a Microsemi SmartFusion2 (SF2) System On a Chip (SoC) FPGA M2S050-FG896. This is a flash-based<sup>3</sup> FPGA which has SEU immune configuration memory, as well as several other radiation tolerance measures implemented [6]. It also comes with a Microcontroller Subsystem which is based on a hardcore ARM Cortex-M3 microcontroller. On Microcontroller Subsystem we are able to build a Linux system, which replace the functionality of the Control System board (DCS)-card. The ProASIC was also not need as a reconfiguration FPGA anymore, but will still be used as a radiation monitor, this part of the RCU2 is now called RadMon, and consist of a ProASIC and SRAM chips. Another issue encountered in the design was that the TTCrx chip that was used for handling the clock and trigger signal on RCU1 was out of stuck and obsolete. This is being replaced by a optical receiver and a limiting amplifier. The limiting amplifier has been tested in this thesis, see section 4.1.7.

One of the limits with the old setup was that the bus between RCU and FECs was to slow. This was fixed by dividing the readout into 4 sections instead of 2, which effectively doubled the readout speed. Therefore all of the backplanes had to be redesigned and replaced.

---

<sup>3</sup>Flash-based FPGA means that configuration registers is saved in flash memory cells. Compared to SRAM-based FPGA where configuration is saved in SRAM cells, flash-based FPGA is much more tolerant against radiation.

# Chapter 3

## Radiation and Radiation effect on Semiconductor devices

Radiation and radiation effects are a known challenge when designing electronics which are going to be used at CERN. There is therefore of highest importance to know about these effect, how they effect the electronics, how much damage they can cause and how we can protect and prevent the radiation effect to do damage.

This chapter is based on references [7], [8], [9], [10] and [11] if not otherwise stated.

### 3.1 Interaction of Radiation With Matter

Radiation is defined as a process which energy in the form of energetic particles or electromagnetic waves is transmitted through a medium or space. Radiation is normally divided into two categories, that is *Charged radiation* and *Neutral radiation*.

Charged radiation consist of charged particles like protons(p), alpha( $\alpha$ ) and beta( $\beta$ ) particles and heavier ions. Neutral radiation consist of neutral particles like neutrons(n) and photons from gamma( $\gamma$ ) and X-rays. Particles which interact with a material will deposit some or all of its energy in the interaction, and can either interact with atoms, electrons, nucleus or the particles inside a nuclei. How much energy is deposited and which of these a particle will interact with is depended on the energy, mass, the charge of the particle and what material it interacts with. One of the main difference between charged particle and neutral particle is that charged particles will be effected by the Coulomb force, that is the attraction or repulsion of

particles or objects because of their electric charge. In the next sections we will look more closely on how a charged particle and neutral particle interact with matters.

## 3.2 Charge particle and their Interaction with Matters

When a charged particle with high speed is passing through a material it will experience multiple elastic and inelastic collisions with the atoms in the material, resulting in slowing down or stopping the particle. When a particle collide with a atom there are several process that can contribute to the loss of energy. They are:

- Inelastic scattering towards atomic electrons
  - Excitation and ionization
- Elastic scattering towards atomic electrons
  - Ramsauer Effect
- Inelastic scattering towards Nuclei
  - Nuclear reaction
- Elastic scattering towards Nuclei
  - Rutherford/Nuclear scattering
- Other processes
  - Bremsstrahlung and Cherenkov radiation

Which of these that contributes to most of the loss of energy is depended on the initial energy, velocity, mass and charge of the particle as well as the properties of the material it collides with. For example, for heavy charge particles(protons or heavier ions), inelastic collisions with the atomic electrons in a material will contribute to most to the energy loss of the particle. A common expression for these processes is called "stopping power".

### 3.2.1 Stopping Power

If we have a particle with a given energy passing into to a material, where  $dE$  is the mean energy that the particle losses by traveling through a path segment,  $dx$ ,

of the material. Then  $-\frac{dE}{dx}$  is the stopping power or also called the "rate" of energy loss for the particle. The stopping power depends on the type and energy of the radiation and on the properties of the material it passes.

The classical expression that describe the stopping power is the *Bethe Bloch formula*, and is written as you can see in equation 3.1.

$$S = -\frac{dE}{dx} = \frac{n_A Z_A Z^2 e^4}{4\pi\epsilon_0 m_e V^2} \left[ \ln\left(\frac{2m_e v^2}{I}\right) - \ln\left(1 - \frac{v^2}{c^2}\right) - \frac{v^2}{c^2} \right] \quad (3.1)$$

$n_A$	Number of atoms per unit volume
$Z_A$	Average atomic number of the material
$Z$	Atomic number of particle
$e$	Electron charge
$c$	Speed of light
$\epsilon_0$	Vacuum Permittivity
$m_e$	Electron rest mass
$v$	Particle velocity
$I$	Effective material ionization potential

### 3.2.2 Specific Stopping Power

Another way of looking at stopping power, is by looking at energy loss as function of mass per area 3.2. Here  $\xi = \rho x$  and  $\rho$  is the density of the material. The extension for specific stopping power is normally given as  $[\frac{\text{MeVcm}^2}{\text{g}}]$

$$S = -\frac{dE}{d\xi} = -\frac{1}{\rho} \frac{dE}{dx} \quad (3.2)$$

From this formula we see that if we are considering two different particles with the same velocity, the only factor that changes is  $Z^2$ . Therefore heavier particles will experience larger energy loss in a material then lighter ones. In figure 3.2.1 we can see specific energy loss for different particles in air. We can see that the value of  $\frac{dE}{dx}$  for different types of particles approaches a near-constant broad minimum value at energies above several hundred MeV, where their velocity approaches the velocity of light.

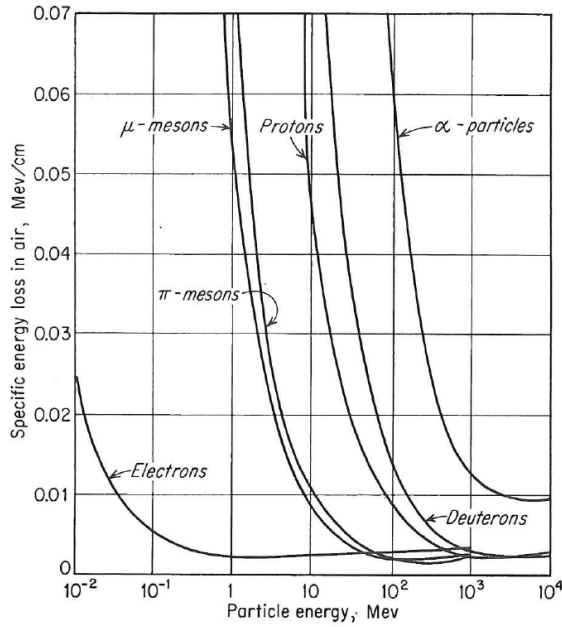


Figure 3.2.1: Variation of the specific energy loss in air versus energy of the charge particles shown

At low particles energies, where charge exchange between the particles and absorber becomes important, the Bethe Bloch formula begins to fail. That is because the positively charged particles will then tend to pick up electrons from the absorber, which effectively reduce its charge and consequently linear energy loss, and will at the end become a neutral atom.

### 3.2.3 Linear Energy Transfer LET

Linear Energy Transfer (LET) is closely related to stopping power of a particle, but instead of focusing on energy loss of the particle, LET focuses on the energy that is deposited in a local volume. For low energies, LET is often said to be equal to the stopping power, even though the particle energy that turn into photons may escape the local area. For higher energies, small particles like ionized electrons can escape the local volume. The local volume is defined by yourself, and can be everything from part of a molecule to a hole organ. One alternate definition of LET can be seen in equation 3.3

$$L_{\Delta} = \left( -\frac{dE}{dx} \right)_{\Delta} \quad (3.3)$$

where  $\Delta$  is the upper energy limit for the secondary electrons included in the calculations. If  $\Delta$  is set to  $\infty$ , all secondary electrons are included in the calculations,

making LET the same as stopping power.

### 3.3 Neutral particle and their Interaction with Matter

#### 3.3.1 Neutrons

Neutrons are subatomic structure that are present in most atomic nuclei. Neutrons carry no charge and can therefore not interact with matter by means of the coulomb force, which dominates the energy loss mechanisms for charged particles. Neutrons can also penetrate several centimeters into matters without any type of interactions, making neutrons hard to detect. When neutrons undergo a interaction, it is with the nucleus of the absorbing material. This can result in total disappearance of the neutron resulting in one or more secondary radiations, or change of the direction of the neutron. The secondary process of neutrons can largely ionizing.

#### 3.3.2 Photons

Photons may appear from gamma rays or X-rays. Photons has as neutrons no charge, and are therefore not effected by the coulomb force, additionally photons has no rest mass and travel in constant speed of light. The energy of a photon is given in the formula  $E = hf$  where f is the frequency of the particle and h is the Planck's constant. There are three main process where a photon may react with matters, they are:

- Photo electric effects
- Compton scattering
- Pair production

### 3.4 Radiation Effects on Semiconductor Devices

Semiconductor devices planned to used in a radiation environment are likely to be effected by the radiation in some way. If not taking properly into account, the radiation effects may damage or even destroy the electronics. Therefore

there is of highest importance to know about how irradiation can effect the semiconductor devices. We normally divide radiation effects in two groups that is *Singel Events effects* and *Accumulative Effects*.

### 3.4.1 Single Events Effects SEE

Single Event Effects are due to the energy deposited by one single particle in the electronic device. Therefore, they can happen in an moment, and their probability is expressed in terms of cross-section [12]. This effects has been an increasing problem as the manufacture process are getting smaller and smaller, making circuits more weak for radiation. In the next sections we will look into three SEEs, that is Single Event Latchup (SEL), Single Event Transient (SET) and Single Event Upset (SEU).

#### Single Event Latchup SEL

A Single Event Latchup (SEL) is phenomena where a low resistance path between power and ground is formed, normally resulting in burned traces, which means reduced performance or destruction of the chip. Therefore it is of highest importance to know about this effect, to know how to counter or to protect from latches in design phase. In a Complementary Metal Oxide Semiconductor (CMOS) process a SEL can occur when a ionized particle penetrate the silicon in a transistor causing a charge to turn ON the parasitic bipolar transistors formed by the substrate, well, and the diffusion. This will result in a low resistance path between power and ground, and a high current will flow. If a SEL has occurred, power to the chip needs to be turned off immediately, before the high current flowing from power to ground will burn interconnections and permanently set the chip out of function.

How a latchup may occur can be understood by looking at a CMOS inverter, see figure 3.4.1. From figure 3.4.1(a) you can see a resistor formed in the well and substrate, and a parasitic bipolar npn-transistor and pnp-transistor formed inside the inverter. An equivalent circuit can be seen in figure 3.4.1(b). Originally both of the bipolar transistors are turned off, and no current flows through the transistors. A latchup can be triggered if a ionizing particle flows into the substrate creating a transient current that can set  $V_{sub}$  high, causing npn-transistor to turn ON. If the npn-transistor turns ON, then current will flow trough  $R_{well}$  causing  $V_{well}$  to go low, and setting pnp-transistor ON. When the pnp-transistor turns ON current will flow through  $R_{sub}$ , causing  $V_{sub}$  to rise, and we have created a positive feedback, causing high current to flow from power to ground.

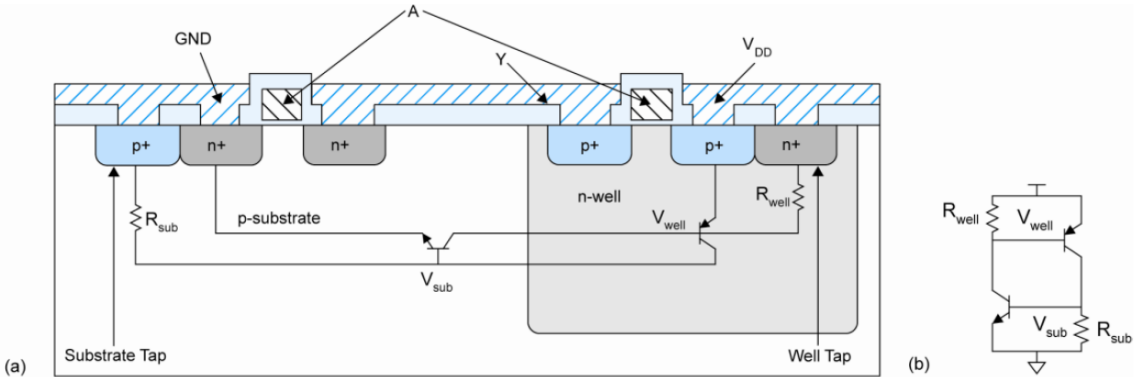


Figure 3.4.1: (a) A CMOS inverter with parasitic bipolar transistors (b) A model of the parasitic circuit

### Single Event Transient SET

Single Event Transient (SET) is a transient pulse of current in a logical path of a circuit. A SET is caused by an ionizing particle leaving a transient current close or on a sensitive circuit node. This current can cause a change of value on that node for a short time, and if this value is clocked in on a register, we will have an unwanted change of value and that is called a SEU. If this value is not clocked out or saved in some way, the current peak will just flat out, and nothing will happen. A way to detect SET could be to make a shift register made up of a known number of register and a known input data. By checking the output and compare with the known value, you can detect if a SET has occurred.

### Single Event Upset SEU

Single Event Upset (SEU) is change of state in a logical element, caused by radiation. This phenomena can often be seen in memory cells or registers, where data is stored. A SEU is a "Soft error", which means that it is a non-destructive type of error. By resetting or overwriting after an SEU has occurred, the error will disappear.

For better understanding of SEU we can look at a six transistor SRAM cell, see figure 3.4.2. If we say that  $Q = '0'$  and  $Q\_b = '1'$ , so there is a value '0' written to the cell. Then a high energetic neutron strikes into the drain of transistor D\_2 and hits a silicon atom. This cause shattering of the atom into charged fragments (ions) that travels through the substrate. These ions leaves a trail of electron-hole pairs, see figure 3.4.3(a). When the resultant ionization track traverses or comes close to the depletion region, carriers (electrons) are rapidly collected by the electric field creating a large current transient (SET) at that node, causing voltage drop at the node  $Q\_b$ . If this voltage drop is high enough, transistor P1 will be opened up, and transistor D1 will be closed, causing  $Q$  to go towards '1' which again causing P2 to

close and D2 to open up causes  $Q_b$  to be discharged through D2, and set to '0'. Then the SRAM cell has changed value from '0' to '1', and we have a SEU.

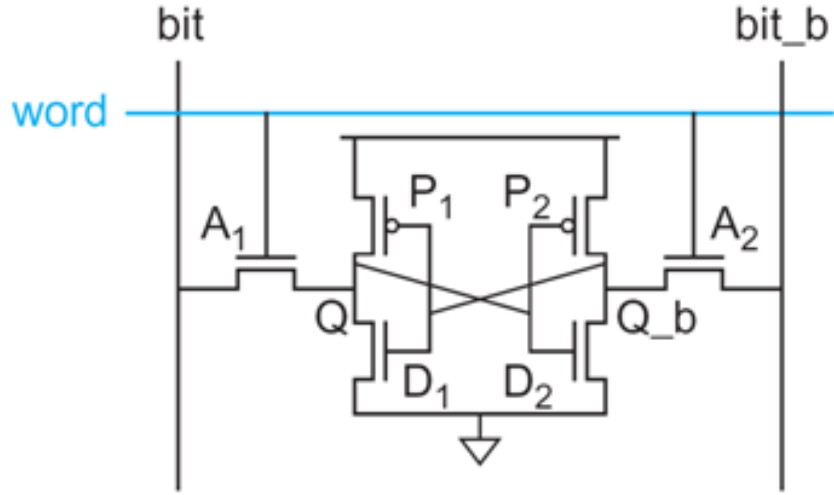


Figure 3.4.2: Six transistor SRAM Cell



Figure 3.4.3: (a) Electron hole pairs generated (b) Carrier are drawn towards the depletion region causing a current jump (c) Additional charge is collected on a more long time scale (hundreds of nanoseconds) [10]

### 3.4.2 Accumulative Effects

Accumulative effects are energy deposition caused by radiation for the whole lifespan of a circuit [12] and [13]. Accumulative effects are measured by the functionality of a device, and power consumption. Some circuits are weak for accumulative effects, and will stop working only after a small dose of radiation, but others device may not even have any effect after a severe dose of radiation. When a chip stops working, we say that it has reached its tolerance level. When we talk about accumulative effects we normally divide into two groups, that is displacement damage, which is a non-ionizing effect, and Total Ionizing Dose (TID) which is a ionizing effect.

## Total Ionization Dose TID

Total Ionizing Dose (TID) is measurement of the dose, that is the energy, deposited in a circuit by radiation in the form of ionization energy. The unit used are Gray (Gy) or rad. The relation between those two can be seen in equation 3.4.

$$1\text{Gy} = 100\text{rad} \quad (3.4)$$

The heart of TID effects is the energy deposition in the silicon dioxide. When ionizing particles penetrates into a transistor, electron-hole pairs will be created. Most of the pairs will recombine shortly after they are generated, but some do not completely recombine because of the electric field. Electrons, with high mobility, can easily leave the oxide, but holes are lower mobility and can be trapped in their point of generation in the oxide. The trapped holes cause a negative threshold voltage shift in the MOS transistor, and if enough holes are trapped, it can result in a transistor which is permanently ON. This phenomena can be seen in figure 3.4.4.

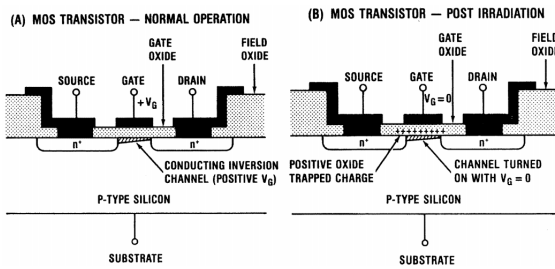


Figure 3.4.4: Layout of a MOS transistor. (A) shows normal operation and (B) shows the transistor after irradiation.

## Displacement Damage

Displacement Damage is a non-ionizing effect mostly induced by low energetic particles colliding with and breaking atoms out of the initial lattice structure of a material. This can affect the functionality of the device. CMOS circuits are normally considered immune to this effect. Displacement damage is not measured in any unit, but it is expressed in terms of the particle fluence, in particles/cm<sup>2</sup>.

### 3.4.3 The TPC radiation environment

The radiation in the LHC is dominated by high energetic neutrons and protons, mostly neutrons with a estimated fluence of  $(0.6 - 1.1) \times 10^{11} \text{ neutrons/cm}^2$ .

Therefore it would be preferable to test our electronics with a neutron beam, but since there are few labs who can produce a neutron beam compared to proton beam most of the electronics is only tested at OCL with a proton beam. There has been done experiment that compares SEU induced by neutrons and protons [14], and the result shows that it is possible to use a proton beam instead of proton beam with small deviations. By comparing a Proton beam with a neutron beam of 21MeV we see that we get 10-25% less SEU cross section for a proton beam compared to a neutron beam. If we increase the energy to 88MeV then we get close to none deviations.

The dose that we could expect for a 10 year period in the ALICE detector is estimated to be approximately 0.6 kRad from Pb-Pb collisions that will be run 1 month a year and a little higher for p-p collisions that will be run 10 months a year [15] and [5]. Therefore we could expect a dose of 1-2 kRad during the time it will be used at CERN.

# Chapter 4

## Preparations for Testing

Testing Integrated Circuits (ICs) is a thing that has been done before when it comes to the design of electronics that are going to be installed in the LHC at CERN. Much of the work presented in this thesis is based on experience from previous thesis [16] [5] [17] [18].

### 4.1 The Integrated Circuits (ICs)

The IC that was tested through this thesis are: TPS51200, MIC69302WU, SN74AVCB164245, SN74AVC2T245, QS3VH257, SY89831, ADN2814, MAX3748, INA210, TLV3011 and SF2 M2S050-FG896. What each of these are, and how these was tested will be discussed in the following sections.

For each of the different IC, except SF2, a Printed Circuit Board (PCB) was made with only the necessary electronics to make it work and to be able to test the functionality of the IC. one to two Connectors was placed on the different PCBs and connected to USB-Data Acquisition (DAQ) boards from National Instruments. These gave us the possibility to control the inputs of each IC and monitor the outputs. A small resistor was placed in serial with the power input, so we would be able to measure the voltage over this resistor to get current.

We wanted to have two PCB for each of the IC that was going to be tested to have more test data on each IC, and to be sure that the error we would see wasn't just a coincidence. There may be some difference between two boards made for the same chip, that is because the first board made may have some modification on the PCB, to make it work. When the second board was made, error or mis functions was fixed in the design before a new board was made. The second version was tested

first, in case we didn't have time to test both of the versions. Later in this thesis the second board that was made are marked with <sub>1</sub> and the first board was marked with <sub>2</sub>. Two of the ICs (ADN2814 and MAX3748) was only made one version of, since we didn't have any spare IC at the time to make a new PCB. All of the test PCBs had a mark on the back indicating the center of the IC, this was used to pinpoint the center during the tests.

To supply and measure everything on the test boards, Data Acquisition (DAQ) devices from National Instruments were used. The DAQ devices we used are called USB-6009, USB-6008 and USB-6501. USB-6009 was used as the main one, and the other were used when needed more digital or analog inputs or outputs. USB-6009 has 8 single-ended analog input (AI) channels, 2 analog output (AO) channels and 12 digital input/output (DIO) channels, and also a 2.5 V and 5.0 V signal. The analog outputs has a limit of 5 mA, but some of the ICs that was tested required more than that. For these cases the 5 V signal was used, that can deliver current up to 200 mA. More information on the DAQs can be seen in the reference [19].

#### 4.1.1 TPS51200

This is a adjustable power regulator from Texas Instruments. It is special designed for DDR RAMs, it can be used for DDR, DDR2, DDR3 and DDR4 applications.

In figure 4.1.1 you can see a schematic layout of the PCB for TPS51200. The PCB was designed after a recommended setup for DDR3 application from the datasheet [20]. Input voltage was set to 3.3 V. Voltage over resistor R1 (See figure 4.1.1) was measured and used to calculate current consumption. Output voltage was also monitored.

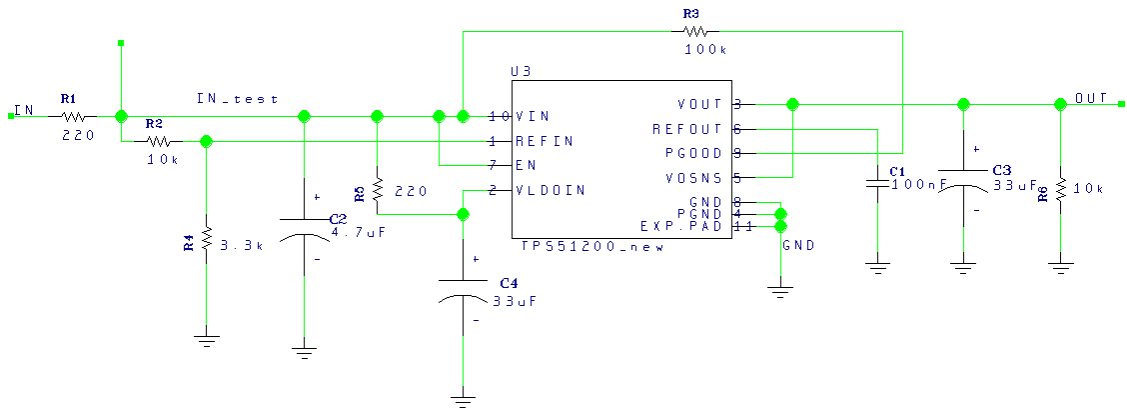


Figure 4.1.1: Schematic for the TPS51200 test board

### 4.1.2 MIC69302WU

This is a ultra low dropout<sup>1</sup> adjustable power regulator from Micrel Incorporation. It is in a family of high current, low voltage regulators, and can deliver a current of up to 3 A. It is a adjustable regulator, which means that by changing R1 and R2(see figure 4.1.2) you can adjust the output voltage, see equation 4.1. For the two test boards that was made we used a input voltage of 3.3 V. Voltage over resistor R?(See figure 4.1.2) was measured and used to calculate current consumption. Output voltage was also monitored. We used 10 kΩ for both R1 and R2 which gave us 1 V on the output.

A third PCB was made with this IC. This was used to supply 3.3V to the PCB that requires more than 5 mA which is the maximum the analog outputs the DAQ form National Instruments can deliver. This was design with resistor values of  $R? = 20 \Omega$ ,  $R1 = 5.6k \Omega$  and  $R2 = 1k \Omega$ , which gives us 3.3 V output. This PCB was used to supply SY89831U, ADN2814 and MAX3748

$$V_{out} = 0.5 \times \left( \frac{R1}{R2} + 1 \right) \quad (4.1)$$

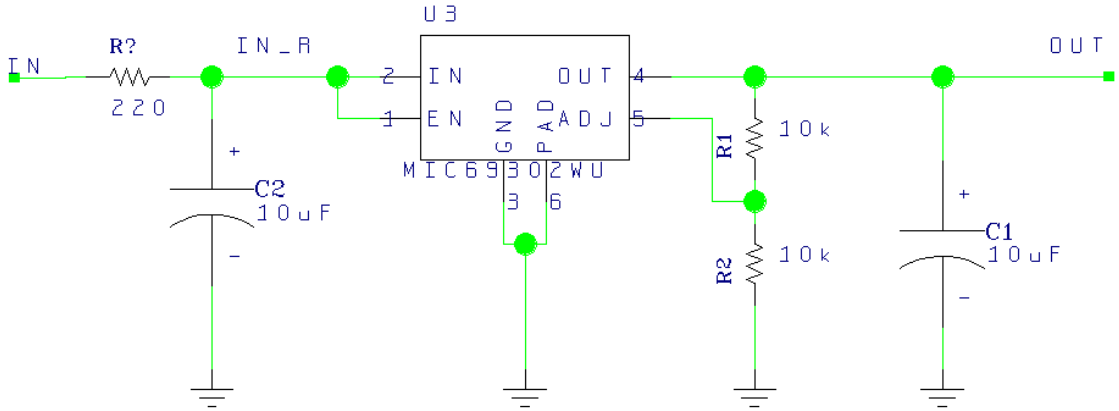


Figure 4.1.2: Schematic for the MIC69302WU test board

### 4.1.3 SN74AVCB164245

This is a 16-bit noninverting bus transceiver, with configurable voltage. Used for level shifting for digital signals. An application example could be to convert a 16-bit digital signal of 1.5 V to a 16-bit signal of 3.3 V. Direction of the signal is decided

---

<sup>1</sup>Low dropout means that voltage on the output can be close up to the input. For MIC69302WU low dropout means that  $V_{IN} - V_{OUT}$  can be as low as 500 mV

by DIR1 and DIR2. The input and output high value can be set to anything between 1.4 and 3.6 V, the low value is set to be 0 V.

For the test board the supply voltages(VCCA and VCCB, see figure 4.1.3) was both set to 3.3 V to make it more simple to test. Voltage over resistor R1 (See figure 4.1.3) was measured and used to calculate current consumption. To make sure that the circuit didn't drag current through the inputs on the chip we used a pMOS transistor that was connected as seen in figure 4.1.3. This made the current for the inputs come from the supply pin, and not from the digital signal IN. The outputs was measured digitally.

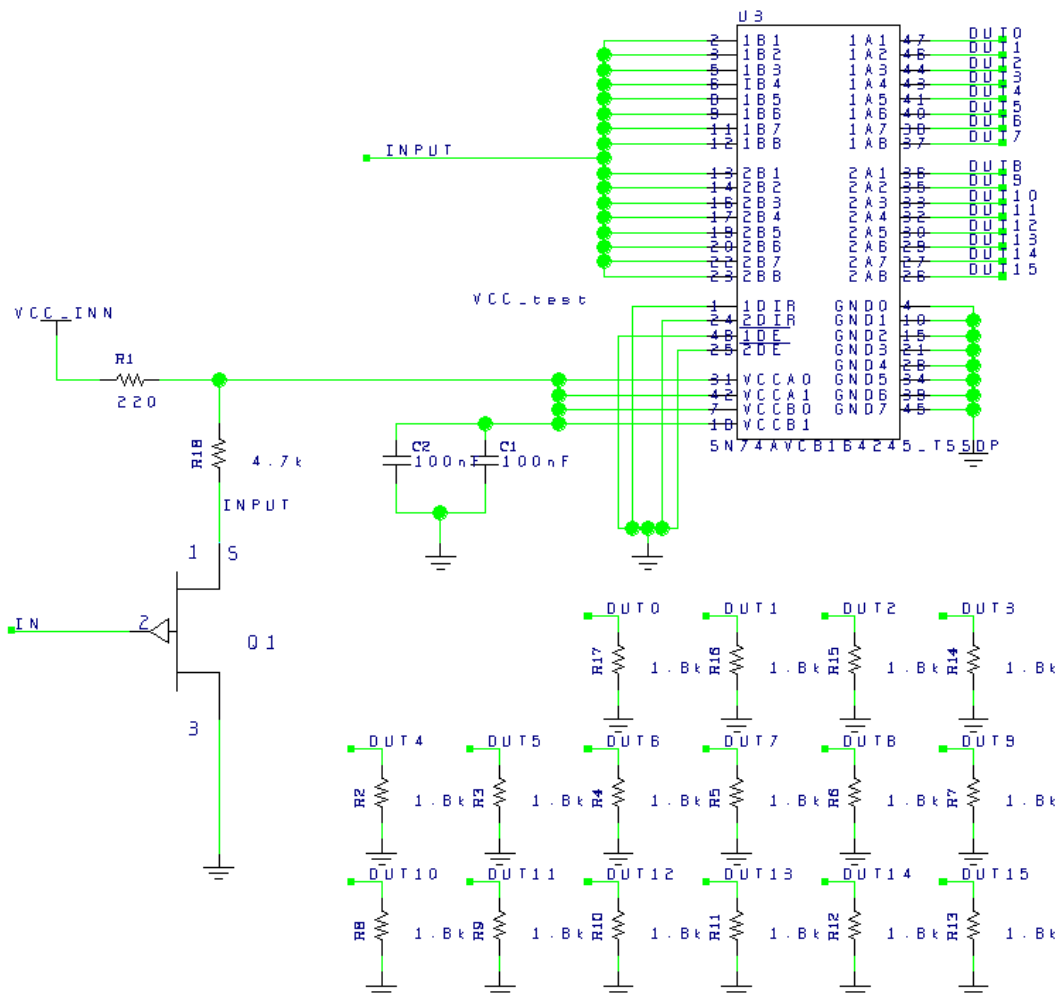


Figure 4.1.3: Schematic for the SN74AVCB164245 test board

#### 4.1.4 SN74AVC2T245

This is a dual-bit noninverting bus transceiver, with configurable voltage. It has the same function as SN74AVCB164245, but this only has two inputs. The input and

output high value can be set to anything between 1.4 and 3.6 V, the low value is set to be 0 V. Direction of the signal is decided by DIR1 and DIR2

As for SN74AVCB164245 a 3.3 V supply was used for both VCCA and VCCB, see figure 4.1.4. Voltage over resistor R1(See figure 4.1.4) was measured and used to calculate current consumption. The output signals was monitored digitally.

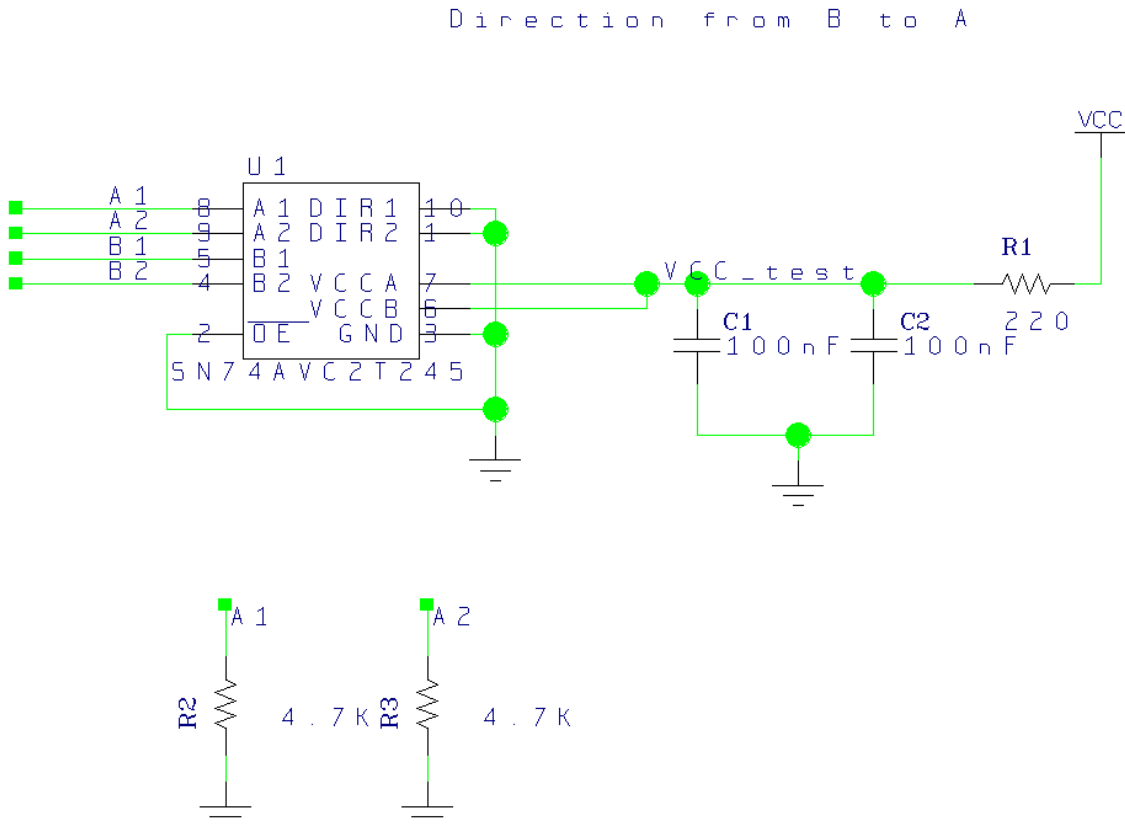


Figure 4.1.4: Schematic for the SN74AVC2T245 test board

#### 4.1.5 QS3VH257

This IC consist of four 2 to 1 multiplexer/demultiplexer. It has high bandwidth, up to 500 Mhz, low ON resistance and high OFF resistance.

Supply voltage was set to 3.3 V. Voltage over resistor R1(See figure 4.1.4) was measured and used to calculate current consumption. For the Select input a analog output signal was used. The input signals was set digitally, and the outputs was measured digitally.

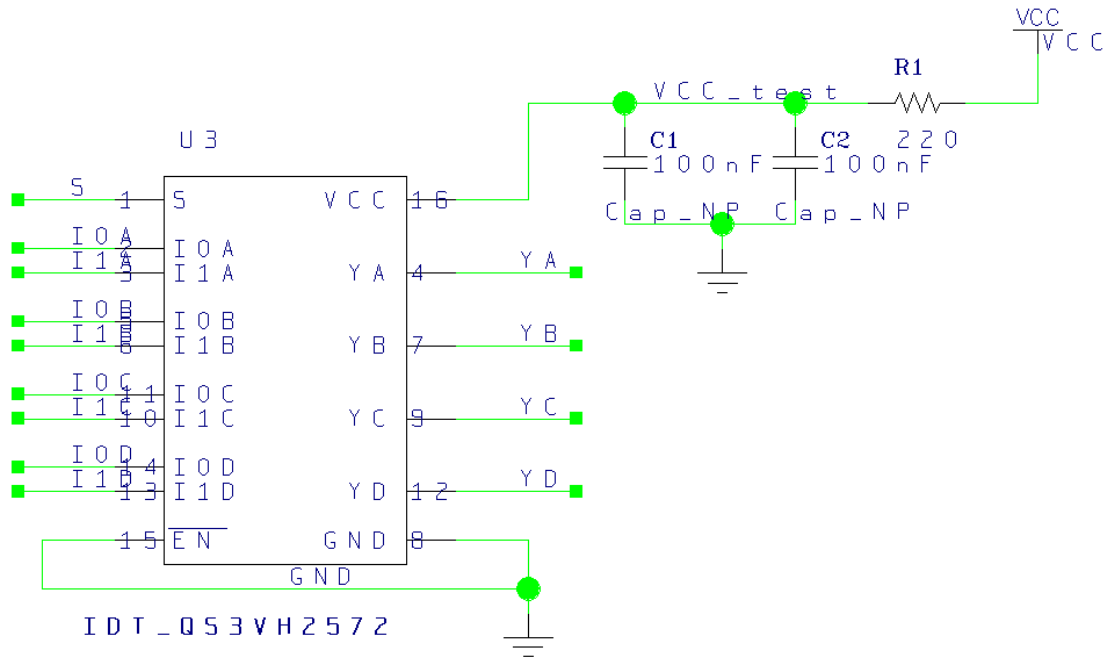


Figure 4.1.5: Schematic for the QS3VH257 test board

#### 4.1.6 SY89831U

This is a high speed, 2GHz differential Low Voltage Positive Emitter Coupled Logic (LVPECL) 1 to 4 fanout buffer optimized for ultra-low skew applications.

The input signal to this IC is differential. The DAQ device we were using doesn't have a differential output signal, so here we had to use a little trick to make it work. We used two single-ended output signal that was set to the opposite of the other, and every 100 ms the values switch, so that when IN+ was 3.3 V IN- was 0 V, and when IN+ was 0 V IN- was 3.3 V. The outputs was measured by the analog inputs of DAQ USB-6501.

This IC requires a large current typically around 60 mA, and we could therefore not use the analog outputs. So we had to use the modified version of the MIC69302WU PCB, that will supply us with a 3.3 V signal up to a current of 200 mA. Current consumption was measured over the input resistor of the MIC69302WU PCB.

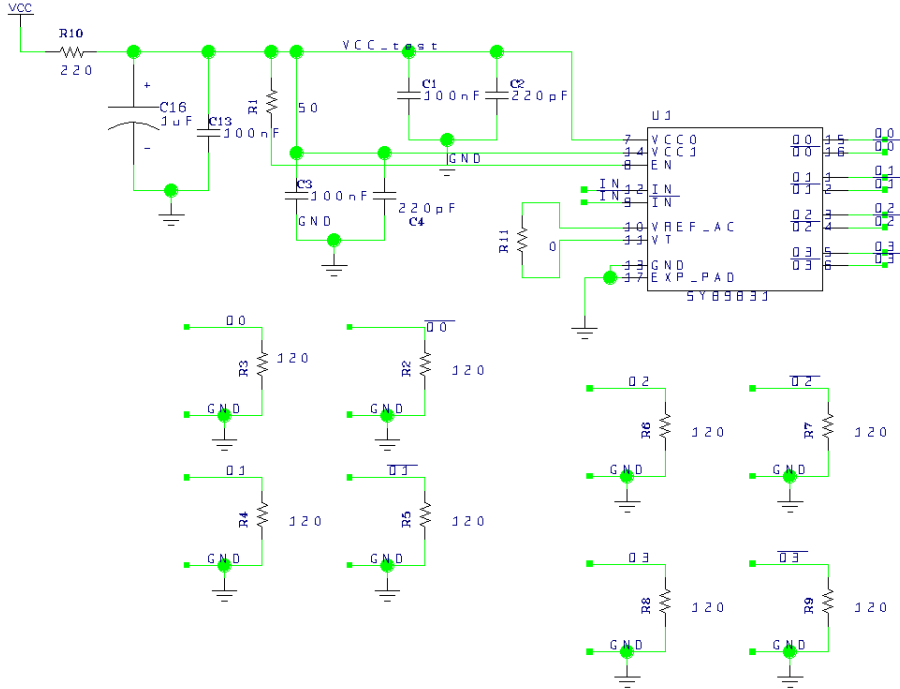


Figure 4.1.6: Schematic for the SY89831U test board

#### 4.1.7 ADN2814 and MAX3748

These two boards are used for the same purpose, and the one of them that performs best will be chosen to be used on the RCU2. ADN2814 is a clock and data recovery IC with integrated limiting amplifier. Works in rate of 10 Mb/s to 675 Mb/s. Gives out a Low-Voltage Differential Signaling (LVDS) clock and data signal. MAX3748 is a limiting amplifier. Works in rate of 155 Mb/s to 4.25 Gb/s. Gives out a Current-Mode Logic (CML) data output signal.

These ICs are going to be used to make a stable LVDS or CML signal from an optical transceiver. The signal from the optical transceiver is a Manchester coded signal consisting of data and clock. There are a few differences between the two ICs. MAX3748 comes in a smaller package and uses less power and works in higher rates, but it doesn't have a clock return function as ADN2814 has. Both work for our specific use, therefore we will see from the test results which one will be used.

The two limiting amplifiers (ADN2814 and MAX3748) required a more advanced input than the DAQ board could give us, and therefore a SmartFusion2 (SF2) starter kit was used in addition to the DAQ. The SF2 board was used to code a clock and data signal into a differential Manchester signal and to decode the differential Manchester signal back to clock and data after it has gone through the ICs. The SF2 was also used to compare the original signal with the signal coming out from the IC.

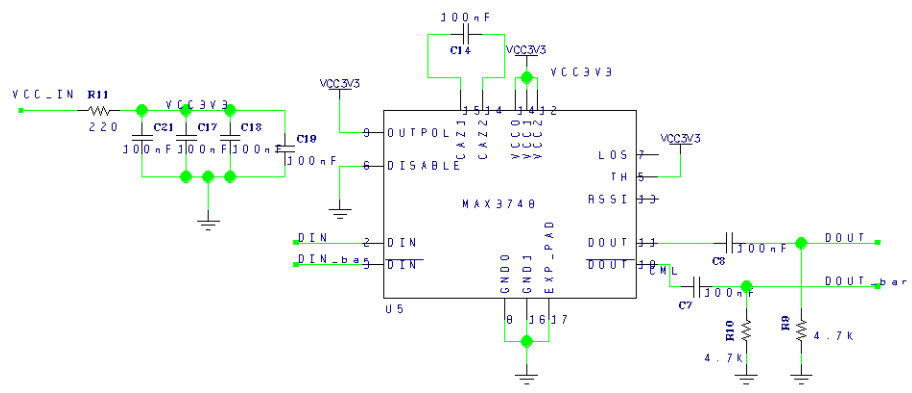


Figure 4.1.7: Schematic for the MAX3748 test board

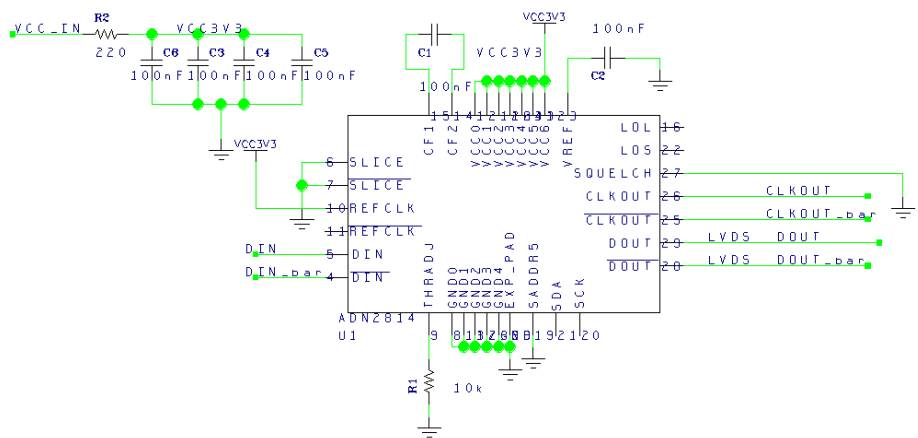


Figure 4.1.8: Schematic for the ADN2814 test board

#### 4.1.8 INA210

INA210 is a so called Current-Shunt Monitor, that is a IC that is used to amplify small current signal into higher voltage signal. This is done by sending the signal that you want to measure current of, over a small resistor, typical smaller than 1 Ohm. Then a voltage will be formed over this resistor and will be amplified through the IC. This IC comes in a family of 5 with different amplifications, the one we are using has an amplification of 200 V/V.

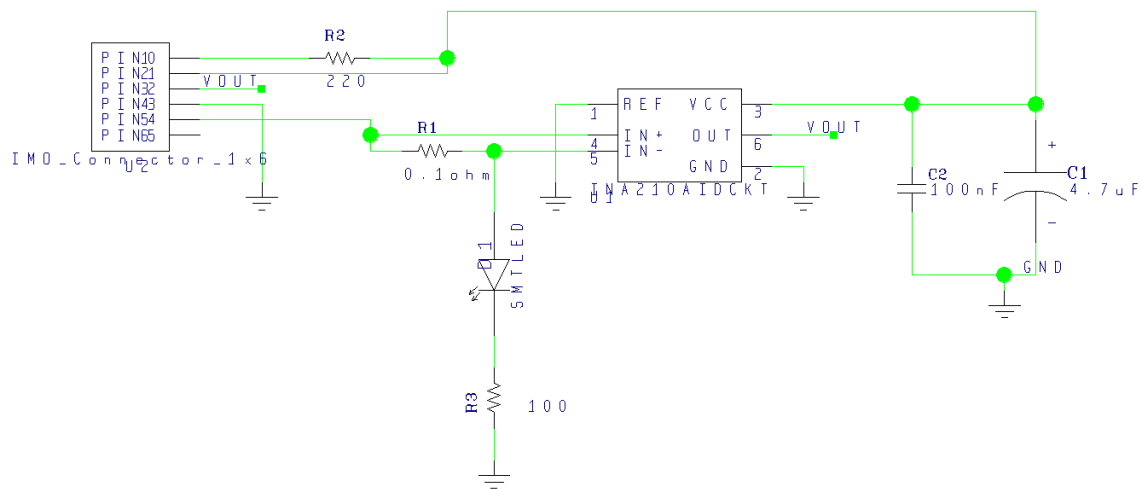


Figure 4.1.9: Schematic for the INA210 test board

#### 4.1.9 TLV3011

This is a comparator with a built in voltage reference of 1.242 V. It supports low supply voltage from 1.8 V to 5.5 V, and has a open-drain output with fast response time. A 10 kOhm resistor is needed as pull-up on the output.

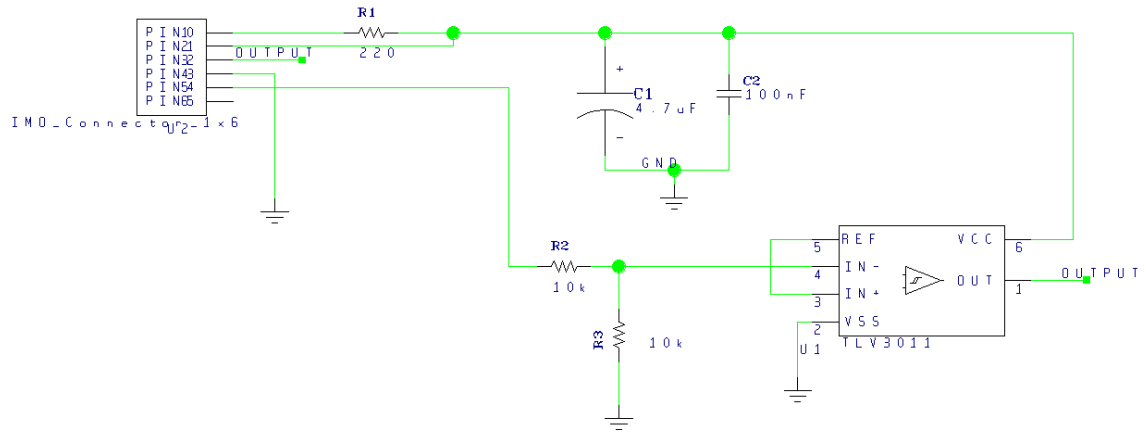


Figure 4.1.10: Schematic for the TLV3011 test board

#### 4.1.10 All the test boards

In figure 4.1.11, 4.1.12 and 4.1.13 pictures of the different PCB boards.

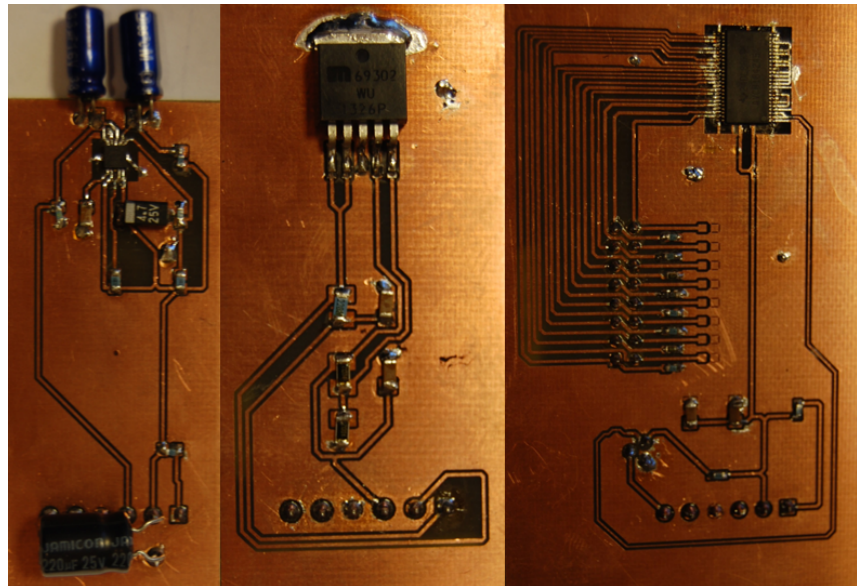


Figure 4.1.11: Picture of PCB boards, from left we have, TPS51200, MIC69302WU and SN74AVCB164245

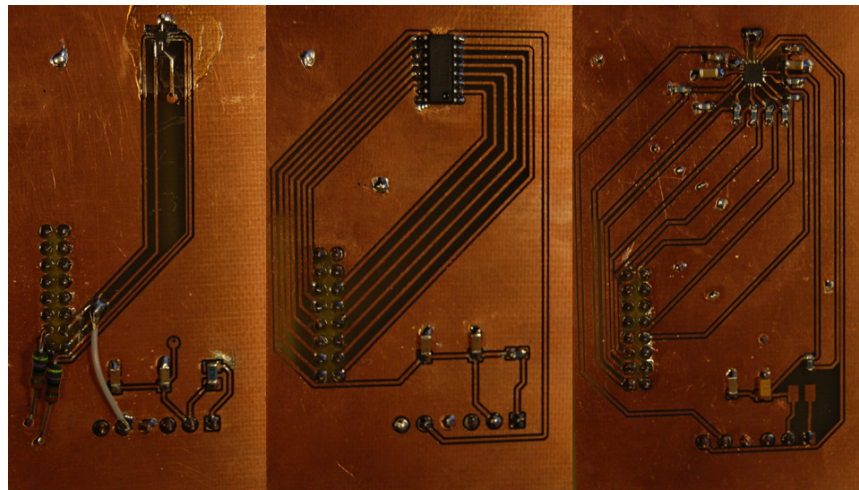


Figure 4.1.12: Picture of PCB boards, from left we have, SN74AVC2T245, QS3VH257 and SY89831U

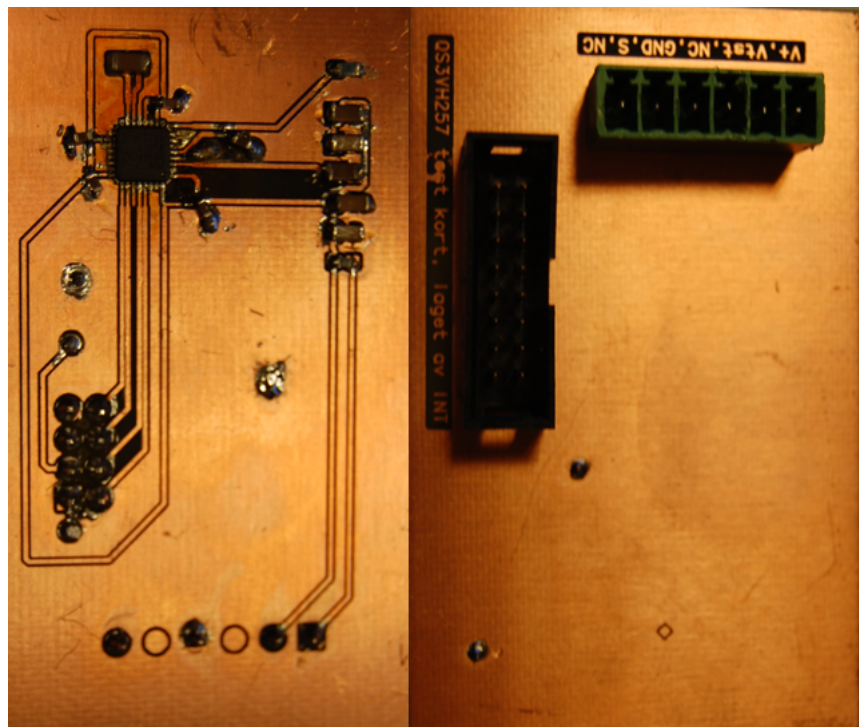


Figure 4.1.13: Picture of PCB boards, from left we have, ADN2814, MAX3748. plus back-side of QS3VH257, you can see the mark at the top indicating the center of the IC

## 4.2 Software

For each of the different test board, a simple labVIEW program was made specially designed to supply and monitor a specific IC under radiation. In these program time from start, current consumption and the status of the output signal (or the output voltage for the regulators) can be measured and monitored. Data is constantly saved in a text file on disk.

In figure 4.2.1 you can see an example of a labVIEW program used for SN74AVC2T245.



Figure 4.2.1: LabVIEW program for SN74AVC2T245

## 4.3 SmartFusion2

SmartFusion2 (SF2) SoC FPGA integrate a flash-based FPGA, a Microcontroller SubSystem (MSS), which consist of a microcontroller, a ARM Cortex-M3 processor, PLLs, bus communication through APB and AHB bus, communication protocols like Ethernet, UART, SPI and  $I^2C$ , and much more. It is also said to have immune configuration memory, as well as several other radiation tolerance measures implemented. We are going to use the package M2S050-FG896, with a FPGA of 56 340 logic elements, 6 PLLs, 1314 kb SRAM, 8 SERDES<sup>2</sup> lanes, and 377 user I/O.

<sup>2</sup>Serilizer/Deserilizer (SERDES) convert data between serial data and parallel interfaces in both direction

Everything one the SF2 that are going to be used in the design has to be tested in some way, unless it has been tested before, or are proven to be radiation intolerant. There are four things that we tested. That is the internal SRAM blocks, the logical element, the PLLs and Single Event Latchup (SEL). How these will be tested will be discussed in the following sections. Other functionality was also tested like Ethernet, SERDES and Clock and data recovery, etc., but these test will not be discussed in this thesis.

### 4.3.1 SRAM test

SRAM cells are as discussed in section 3.4.1, sensitive for radiation. It is important to know how well these work in high radiation areas, so we can know how reliable these are when used. The SRAM blocks on the SF2 are divided up into 72 micro SRAM blocks with a size of 64 x 18 bits, and 69 Large SRAM blocks with a size of 1024 x 18 bits. Both micro SRAM blocks and large SRAM blocks are so called two port SRAM, which means that we can access two addresses at the same time.

The way the SRAM memory was tested is divided into 3 state in a state machine, this can be seen in block diagram in figure 4.3.1. The first state is a reset state, where all values are set to its nominal value. That means all counter is set to 0, write address is set to 0, read address 1, and write data is set to 1010...1010. Read address is always set be one higher then read address.

The next state is a initial state where all addresses are written to. Write data is switched opposite every address increment, so the written data is switched between 1010...1010 and 0101...0101 every other address. When the last bit is written to, the first bit is read.

The last state is a state where all of the addresses are written, read and compared through a endless loop. The data written to a address is always opposite of the previous value on that address, that is to prevent having stuck bits. The state machine will stay in this state until a reset is pushed or power is shut down.

The SEU counter value for both the micro SRAM and the Large SRAM, as well as number of cycles through all addresses is saved in registers and sent to the Microcontroller SubSystem (MSS). These register is saved with Triple Module Redundancy (TMR), that means that the values are saved in three registers, and the majority of these is used. How the data is monitored and checked is discussed in section 4.3.4.

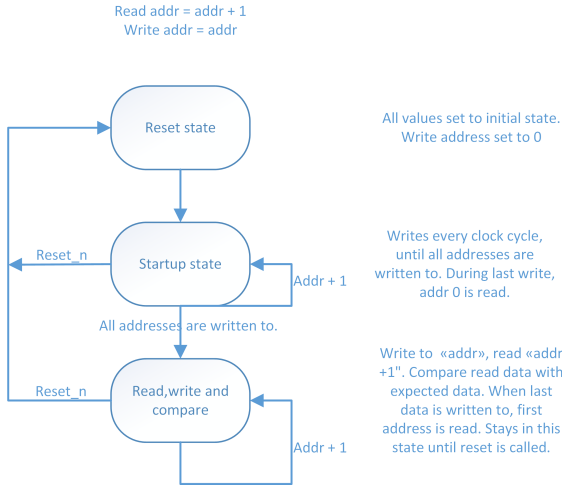


Figure 4.3.1: Flow chart for test procedure of SRAM

### 4.3.2 Test of the Logical element

A logical element consist of a 4 input Look-Up Table<sup>4</sup> and a separate flip-flop which can be used independently from the Look-Up Table. That means that we have 56 340 flip-flops and 56 340 Look-Up Tables available for our design. When a logical element is exposed to radiation, a Single Event Transient (SET) can occur all over the chip. If this happens in the logical element or in the interconnections between logical element, the transient current will normally just be there for a small amount of time, and then it will flat out, causing no error or bit flip in the chip. But if this transient current hits a sensitive node as the input to a flip-flop, or a node that may lead to a change of value at the input, and the input is then clocked out to the output, we would have a unwanted bit change or a so called Single Event Upset (SEU).

The way we tested the logical element is based on [21], which has done a study on how to test FPGAs in a good manner. A good overview of the design can be seen in figure 4.3.2. The idea is to make a long serial chain of flip-flops, otherwise referred to as a shift-register, where a transient can be picked up and make a SEU. By adding a even number of inverters in between each flip-flop we increase the area where an transient can occur, without changing the logic. A known pattern is added to the input of the shift-register, this can be change depending on how advanced you want to be, but typical pattern could be even other '1' and '0'. To be able to operate at high speed, we are using something called Windowed Shift Register (WSR), which takes out the last n-bit of the shift register, and sends it out in parallel, with a frequency n times lower than the original frequency. To check the outputs for errors, the WSR bits will be sent through the I/O-pins to another SF2 starter kit, hereafter referred to as the monitoring board, where data is checked

---

<sup>4</sup>An n-bit Look-Up Table can encode any n-bit Boolean function by modeling such functions as truth tables

for errors. To be able to synchronize the two board, a reset signal and shift enable signal will be sent from the monitoring board to the test board, and a WSR enable signal will be sent from the test board to the monitoring board.

We made generic of all the variables like number of shift-register chains, numbers inverters in between each flip-flop, numbers of bits taken out in the WSR output and the length of the shift-registers. Typical value used is respectively 4,4,4 and 2000.

We wanted to be able to change the clock frequency without reprogramming the FPGA, to see how the frequency effects the number of upset detected. Clock Conditioning Circuit (CCC) which consist of a PLL, multiplexers and divider circuit, are used to configure clock signals on the SF2. The CCC can be configured through a register, so the frequency can be changed without reprogramming the FPGA.

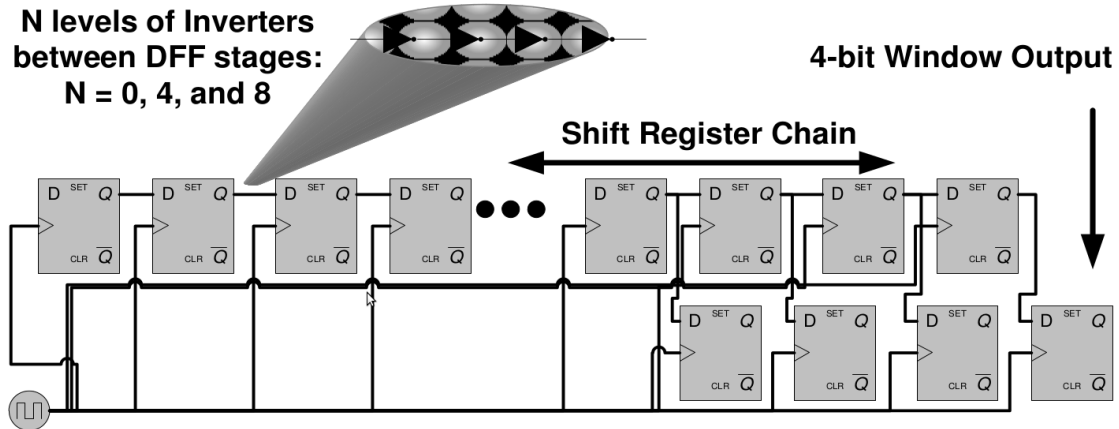


Figure 4.3.2: Flow chart for test procedure of SRAM

### 4.3.3 Single Event Latchup and PLL

A Single Event Transient (SET) is a short circuit between power and ground. If that happens on any spot on the chip, an increase in the supply current can be detected. So the way a SET will be checked, is by constantly checking for increase in current consumption on the chip. A SET will normally destroy a chip, if not counted by shutting power off immediately after the latch has occurred. That is why a separated PCB was made to measure the current, and to be able to shut down the board if a latch is detected. See section 4.3.4 for more information on the board.

The PLLs on the SF2 has a lock signal which goes high if the PLL is in sync with the input. To check if we have a reliable clock signal, the lock signal was sent to a I/O pin and over to the monitoring board, where the lock signal was constantly checked for a falling edge.

#### **4.3.4 Configuration and Monitoring**

To avoid using too many starter-kit and to save time when we were going to test, we implemented all tests into a single project. The test board was communicating with a computer through a serial port, a current measurement board was connected with wires to measure current, and another starter-kit (monitoring board) was connected to the GPIO pins to be able to control and check the Logical element design. More detail of the different test programs and boards used to test the SF2 is discussed in the following sections.

#### **Microcontroller SubSystem and labVIEW**

The Microcontroller SubSystem is used to make a two way communication between the SF2 chip and a computer. On the SF2 starter-kits there is a serial communication from a USB-connector to a UART port on the SF2s microcontroller SubSystem. Values like the SEU counter and cycle counter which is saved in register in the FPGA are sent to the microcontroller SubSystem through APB bus. A C-code was written to the microcontroller, which in short sets up the UART communication and constantly sends SEU counter and cycle counter values through through UART, and checks for received data. The received data is used to determine the frequency. On the computer a labVIEW program was written to receive the data, and show the newest values for a user. Through this program you are also able to select some specific frequencies, by use of pushbuttons in the program, by pushing a button a request to change frequency is sent to the microcontroller. When the microcontroller receives the request, it access the register controlling the *Clock Conditioning Circuit*, and changes to the frequency, by accessing the clock divider.

#### **Monitoring board**

As said in section 4.3.2 a second starter-kit, called monitoring board, was used to be able to monitor and control the *Logical element test design*. On the monitoring board there is a linux system running. A VHDL code is built on the FPGA which takes inn wsr data and wsr enable from the test board and sends out reset, shift enable and pattern. All of the output data is controlled and input data is monitored through APB bus to the linux system. The wsr enable signal tells us when a new data is sent from the test board, when this signal goes high, the wsr data signals is clocked in a register on the monitoring board. The wsr data is then compared with the correct value, and if an error has occurred, a counter will be incremented. The counter value is read in the Linux system.

## Current measurement board

To measure the current into the SmartFusion2 starter-kit, a PCB was made with a microcontroller, serial to USB converter (FTDI chip), some debugging LEDs, power switch, and all the necessary electronics to make all this work together. The microcontroller used is a Texas Instruments MSP430AFE253. That is a 16-bit microcontroller with internal 24-bit ADC. It has an internal frequency of up to 12 MHz, and support high frequency crystal up to 16 Mhz. Two types of serial communication interface are available, that is USART and SPI. Since the microcontroller only has a 16-bit architecture, only 16-bit of the ADC is accessible at a time. The microcontroller has 3 differential ADC inputs, which means three different currents can be measured. A current is measured by adding a small resistor of known value in series of the signal you want to measure current of, and by measuring voltage over the resistor you can calculate the current, by using ohms law ( $I = \frac{U}{R}$ )

To measure current for the SF2 starter-kit a small resistor of 0.1 Ohm was placed in series with the 1.2 V supply voltage, and a 0.16 Ohm resistor for the 3.3 V supply voltage. The voltage over these resistor was measured with the ADC, and the ADC data was sent over USART port to the serial to USB converter, and further to a computer. On the computer a labVIEW program was set up to receive data through the serial port, and when data is received, the ADC value and the known resistor value is used to calculate the current. The current value is constantly saved and exposed for a viewer.

The 3.3 V regulator on the SF2-starter kit has a enable signal, where a pull-up resistor to 5 V is placed, one of the outputs on the microcontroller is connected to this pin. If the current on one of the supply voltages goes over a certain threshold, the bit on the microcontroller is set to go low, resulting in turning the 3.3 V regulator on the SF2-starter kit off. The 3.3 V is used to power all other regulators, so by turning this regulator off, the whole starter-kit turns off.

Schematic, PCB layout and instructions on how to use this board can be found in appendix

## 4.4 Equipment used for testing

Under a radiation test, some equipment are needed. In the following sections some of the equipment used under a radiation test are presented.

#### 4.4.1 SRAM detector

The SRAM detector boards are made by Arild Velure, as part of his master thesis [18]. It is a SRAM-based radiation detector. By checking SRAM chips for SEU, we can find the fluence<sup>3</sup> of the beam.

The SRAM detector is a PCB with a flash-based FPGA, four 16 Mbit Cypress SRAM chips, connectors and supporting electronics. The board can be connected to a computer through a Opal Kelly XEM3001 board, which converts RS485 signal from the FPGA to USB. A labVIEW program has been built specially for this board. From this program we are able to reset data, do some basic settings, and monitor data. The program also constantly saves data onto the disk. The board also has an optical input for scintillator counts, so we could use this board as a scintillator counter as well.

In figure 4.4.1 you can see how the labVIEW program looked like. From here we can monitor SEU on all the 4 SRAM chips, see scintillator counts, reset counters, see time from start as well as other things. SRAM1-10 as you can see on the left side, is different SRAM-board, the board we used was SRAM6.

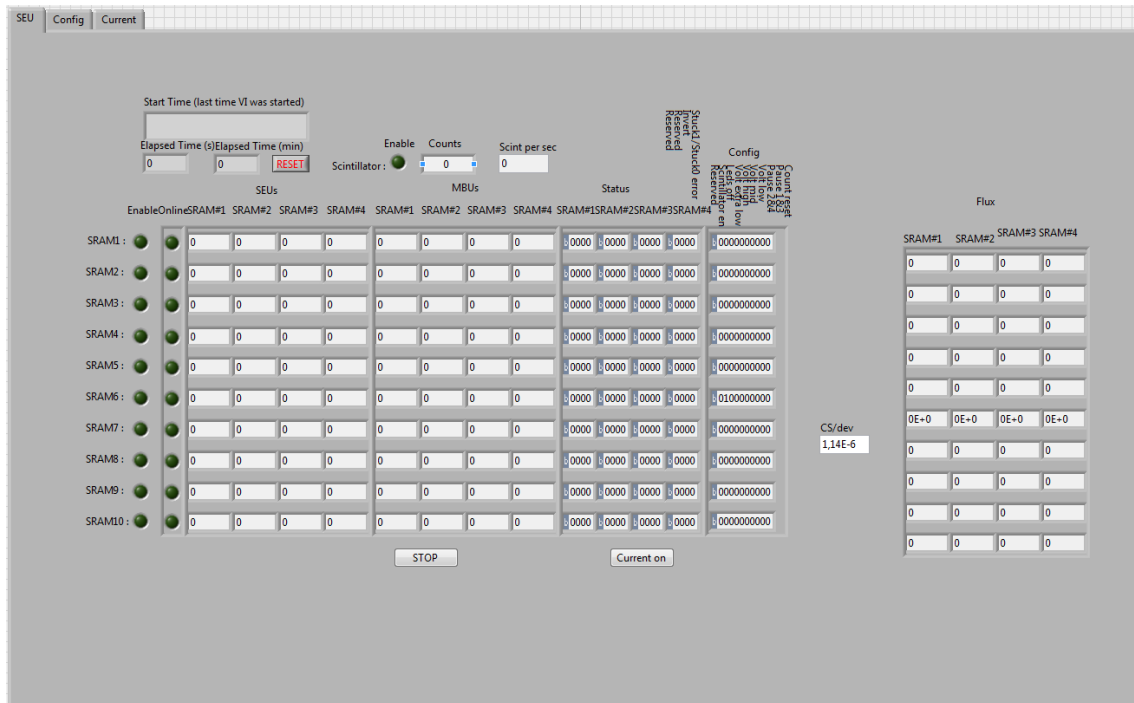


Figure 4.4.1: LabVIEW program for the SRAM

The approach for detecting an Single Event Upset (SEU) on the SRAM is rather straight forward, as can be seen in the flow diagram of figure 4.4.2. There is an

---

<sup>3</sup>Fluence is the total number of particles that intersect a unit area in a specific time interval of interest, and has units of *particle/cm<sup>2</sup>* (number of particles per meter squared)

initial startup phase where a known pattern is written to all the addresses in the SRAM. When the startup phase is done, the value from the first address is read and compared with the correct value, and if one or more of the bits are not equal a SEU has occurred, and a counter will be incremented for each bit at the address which has suffered a upset. After the read, a new value is then written back to the address and the system moves on to the next address. A checkerboard pattern of alternating ones and zeros, is used when writing to the SRAM. To check for stuck bits, the bit pattern is inverted for every cycle through all addresses.

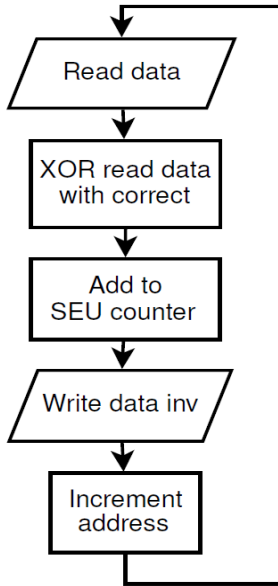


Figure 4.4.2: Flowchart for SEU detection

The cross section (the probability that a incoming particle will induce an SEU) is known, and is found to be to be  $1.14 \times 10^{-6} \text{ cm}^2$  [18] for protons. by measuring SEU under radiation, we are able to calculate the fluence of the beam, since the cross section is known.

#### 4.4.2 Scintillator counter

A scintillator is a material that emits light when it is exposed to ionizing radiation [7]. A scintillator can be used as a stand alone equipment, but then only to detect that there are radiation, by seeing that it lights up. To get a more accurate measurement, we will need a PhotoMultiplier Tube (PM-tube), which has the ability to converts light pulses to current pulses by an electron avalanche process. The current pulses can be detected by a edge counter, which count every falling or rising edge of a signal.

#### 4.4.3 X-Y-positioning system

The X-Y-positioning system is a displacement system where things (for example a PCB) can be mounted and be moved up, down and sideways in a small area controlled by a computer. Communication is done through a serial port and a labVIEW program is used to control the system.

This was used when doing the beam profile as discussed in chapter 5.1.3. In figure 4.4.3 you can see a picture of the front and back of the X-Y-positioning system, with the SRAM detector mounted.

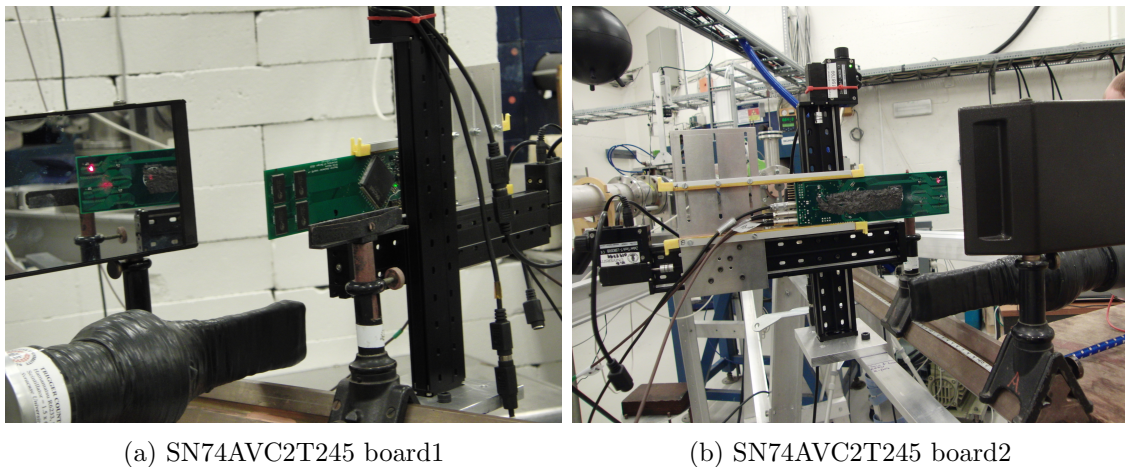


Figure 4.4.3: X-Y-positioning system upfront and behind, with SRAM-board mounted

# Chapter 5

## Irradiation test setup

Irradiation test for the RCU2 electronics which was discussed in the previous chapter, was executed at two facilities, that is Oslo Cyclotron Laboratory (OCL) and The Svedberg Laboratory (TSL). This chapter will give a brief introduction to the two facilities, and explain how we prepared ourself for test and the setup used.

### Purpose of tests

The purpose of testing the RCU2 electronics for radiation is to see if the tested IC are able to survive in a radiation hard environment as we will find in the TPC, see section 1.1. To test the limit for each of the ICs, the ICs was irradiated until a error was detected, current consumption drastically increased or the IC received a much higher dose than was required without error.

### 5.1 Irradiation on OCL

#### 5.1.1 About OCL

Oslo cyclotron Laboratory is located at the Department of physics at the University of Oslo, and was opened in 1978. The cyclotron is of the type MC-35 and was made by Scanditronix AB from Sweden. This is the only accelerator in Norway for ionized particles used in basic research. The cyclotron can accelerate protons, deuteron,  $^3He$  and  $^4He$ , with energies and intensities as seen in the table 5.1 bellow. A drawing of the lab can be seen in figure 5.1.1. The laboratory is divided in tree; the control room, the inner experimental hall and the outer experimental hall. The

cyclotron is placed in the inner hall, and a beam is sent through pipes to the outer hall. There is vacuum inside the cyclotron and the pipes, so that you should not suffer energy loss from collision with air molecules. With magnet you are able to regulate the beam to your desired pipe exit. There are also several cups put on the pipeline which makes it possible to block the beam. These can be used to stop the beam during an experiment, so you are able to go into the experimental area and do changes on your setup. When the cyclotron is running and the beam is on, you are not allowed to enter the inner experimental area.

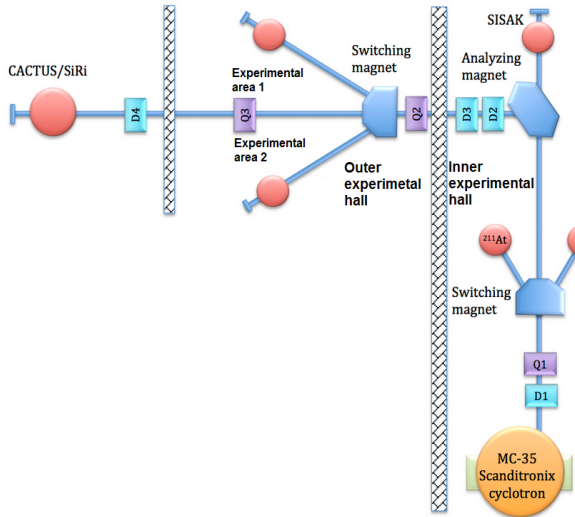


Figure 5.1.1: Out-lay of the OCL

Ionized beam particle type	Energy(MeV)	Intensity( $\mu\text{A}$ )
Proton	2-35	100
Deuteron	4-18	100
$^3\text{He}$	6-47	50
$^4\text{He}$	8-35	50

Table 5.1: Ionized beam particle data table

### 5.1.2 Experiment setup and equipment

The experiment setup was placed in the outer experimental hall in experimental area 2. The experimental setup as well as the equipment used can be found in the figure and table bellow. The equipment was kept in close to the same height around 140-150cm. Beam exit was in a height of 141.5cm.

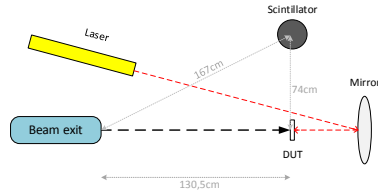


Figure 5.1.2: Experimental setup seen from above

### 5.1.3 Preparation and characterization of the beam

Before we could start testing of the PCB, the cyclotron had to be made ready for a proton beam and the magnet controlling the direction had to be put in the right position to get the beam out in experiment area 2.

#### Beam setup

When we were ready to start the beam test, we had to start with characterization of the beam. The first thing to do is to get an understanding of the beam, and see that it hits around the area that we expect. This was done by using radiation films that turns black when exposed to radiation. One of these was placed right in front of the beam exit and one in front of Device Under Test (DUT) area. This was done to see how the beam spread out, and to get a feeling of where the beam center was. A more precise calibration was done by the use of the SRAM detector and the scintillator. By measuring the relation between scintillator counts on the scintillator which was in a locked position and SEU on the SRAM that was connected to the XY-position system (which made the SRAM freely to move), we were able to find a more precise position of the beam center by seeing which position gave us highest

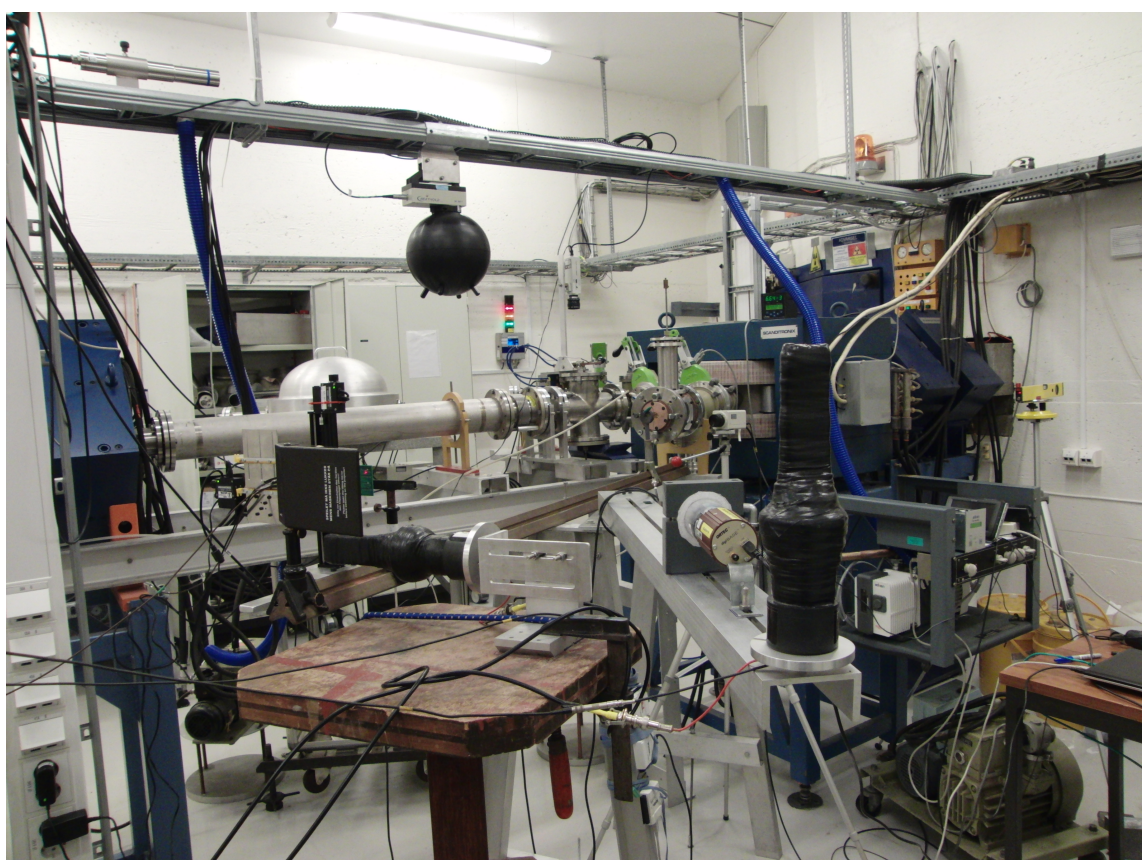


Figure 5.1.3: Picture of the experimental area

Equipment	Explanation
Scintillator	A plastic scintillator with photomultiplier. Was used to measure relative radiation. We had two of these, one that was placed right under Device Under Test (DUT) and one that was placed 75cm away from DUT.
High voltage regulator	Voltage for the photomultiplier. 800V was used.
The test boards	TPS51200, MIC69302WU, SN74AVCB164245, SN74AVC2T245, QS3VH257, SY89831U, ADN2814, MAX3748, INA210 and TLV3011.
SRAM detector	A PCB board with 4 SRAM cells that was used to characterise the beam and to measure scintillator counts
SF2 starter kit	A starter kit board with the SmartFusion2 (SF2) SoC FPGA.
Computer	A VNC server was set up on a computer inside the experimental hall, this made us able to control the experiment from the control room. The computer was running all the necessary software to control and monitor the experiment.
USB DAQ	Data acquisition board form National Instruments(NI). Used to establish analog and digital connection to the test boards and send data to the computer.
Radiation film	A film that reacts when irradiated. Used to identify the beam.
leveled laser	Was used to pinpoint the center of the beam.
Mirror	Used to reflect the laser beam to the backside of the test boards.
XY-positioning system	Connected to the computer so we can change the position of the test boards from a computer

Table 5.2: Equipment used in the experiment

SEU counts compared to scintillator counts. When the beam center is found and everything works as it should, the laser was placed in a position so that the laser beam points to where we had found center of the beam to be. After that we could replace the SRAM board with the PCB that we were going to test. This had to be done every day at startup, before we could start the actual tests.

We were able to control the intensity(Current) of the beam freely from the control room inside the limitation of the beam (for protons that is up to 100  $\mu\text{A}$ ), but we kept us in the area between 100 pA to a few nA. This way the radiation dose to the test boards can be controlled. The beam intensity could be measured by putting a Faraday Cup(FC) in front of the beam. But the FC had to be removed when tests were running, since it will block the beam.

We were running 3 labVIEW programs at all time through the experiment, one for controlling the XY-position system, one for the SRAM board(to measure SEU and scintillator counts when calibrating and to get scintillator counts during the tests) and one program for each of the test boards. The SRAM and test board programs were constantly saving data on the disk.

#### 5.1.4 What was tested at OCL

We had beam time in three periods at OCL, that is 13.11.13-15.11.13, 28.11.13-29.11.13 and 25.03.14-28.03.14. The boards that where tested the first time are: *TPS51200<sub>1</sub>*, *MIC69302WU<sub>1</sub>*, *SN74AVCB164245<sub>1</sub>*, *SN74AVC2T245<sub>1</sub>*, *QS3VH257<sub>1</sub>* and *SY89831U<sub>1</sub>*, tested in that order. The second time, we started with two limiting amplifier IC, since these hadn't been tested before. So the order the PCB was tested the second period was: *ADN2814*, *MAX3748*, *SY89831U<sub>2</sub>*, *TPS51200<sub>2</sub>*, *MIC69302WU<sub>2</sub>*, *SN74AVCB164245<sub>2</sub>*, *SN74AVC2T245<sub>2</sub>* and *QS3VH257<sub>2</sub>*. The third time at OCl, the focus was mainly the SF2 SoC FPGA, but *INA210<sub>1</sub>*, *INA210<sub>2</sub>*, *TLV3011<sub>1</sub>* and *TLV3011<sub>2</sub>* was also tested.

## 5.2 Testing at The Svedberg Laboratory (TSL)

The main difference between OCL and TSL, is that TSL are able to produce beam of much higher energies. The setback with TSL is that it is quite expensive to rent, but then again, the test process is much easier, and there are more people there that can help us if needed. OCL has been rented for free.

### 5.2.1 About TSL

TSL is an accelerator facility belonging to University of Uppsala in Sweden, [22]. It is mainly used for proton therapy of cancer patient by Uppsala University Hospital, but is also used for medical research and radiation testing of electronics. The heart of the installation is a Gustav Werner cyclotron that delivers a beam of charged particles in energies up to 192 MeV. The particles that can be delivered are everything from protons to highly charged xenon ions. There are several extraction points from the cyclotron, which of these that are open can be controlled from the control room. The experiment area for electronics testing, is the the *blue hall*, here there are two extraction points, one used for protons, and one used for neutrons and heavier ions, see figure 5.2.1.

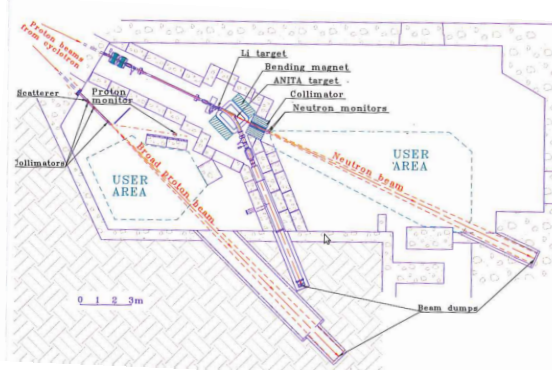


Figure 5.2.1: Layout of the Blue hall

### 5.2.2 Beam setup procedure

At TSL we didn't have to get a beam characterization as we did at OCL. In the Blue hall there is a permanently setup with detectors and a well defined beam line. We only needed to place our test equipment in the blue hall at a given beam point, and start the test. The center of the beam was found by lasers places in looked positions around the hall, one for horizontal direction and one for vertical direction. The head of the laser was movable, so we could point the laser beams towards our

test board. A computer which was remotely controlled through network connection was placed in the hall. This computer was used as a connection point to our test boards. We sat in a room called counting room, where we were able to switch the beam on and off as we desired. There were also a machine in the counting room, which was connected to detectors in the blue hall telling us the fluence (number of protons per  $\text{cm}^2$  in total) of the beam. The fluence can be used to calculate the dose. The energy of the proton beam we had was 180 MeV.



Figure 5.2.2: Setup in the blue hall. Here the RCU2 is mounted, ready for test

### 5.2.3 What was tested at TSL

The main thing that was tested was the SF2 SoC FPGA, we also tested some optical receiver and a detector data link used to send data out of the RCU2. We brought with us two RCU2s and a total of 7 starter-kits, where 3 of these was with a smaller package, M2S050-FG484, and the rest was engineering samples versions of M2S050-FG896, which is the one used on RCU2. For the test discussed in section 4.3 we only used the SF2 starter-kits, since it was only internal test. Two of the starter-kits with the smaller package was tested M2S050-FG484, and one with engineering sample M2S050ES-T-FG896. The RCU2 boards was also irradiation tested, but then other stuff like SERDES (DDL), trigger, clock and data recovery (CDR) and PLL was tested, which will not be discussed thoroughly in this work. Current was measured on both the SF2 starter-kits and RCU2 boards when they were irradiated to check for latchups.

# Chapter 6

## Calculations and Results from Beam Test

*This chapter will explain how the collected data after a radiation test at OCL was used to calculate flux and dose. And results from both irradiation tests at OCL and TSL will be presented.*

After a irradiation test at OCL, the collected data consist of the exposed time, scintillator counts, current consumption and output data of the DUT. From the calibration before radiation test, we got the relation between scintillator counts and SEU on the SRAM detector. From earlier tests with the SRAM detector the cross section for a incoming proton to induce a SEU is known. These data is used to calculate our way to the received dose for each of the different IC. The next section will explain the calculation process.

### 6.1 Calculation of dose

Two ways to calculate dose will be discussed in this section, that is manually using energy loss and LET, see section 3.2, and using simulation data from a program named FLUKA. Which of these gives us the most reliable result will be discussed at the end of this section.

### 6.1.1 Definitions

Absorbed radiation dose has the unit of energy/mass and the SI-unit is gray (Gy), which is 1 Joule of energy absorbed in a kilogram of matter[J/Kg] 6.1. Another unit which is often used when it comes to radiation of electronics is Rad, which is short for "Radiation absorbed dose". The relation between Rad and Gy can be seen in 6.2.

$$1\text{Gy} = 1 \frac{\text{J}}{\text{kg}} \quad (6.1)$$

$$1\text{Rad} = 0.01\text{Gy} = 0.01 \frac{\text{J}}{\text{kg}} = 10^{-5} \frac{\text{J}}{\text{g}} \quad (6.2)$$

The particle energy is normally expressed in electronvolt (eV) or Megaelectronvolt (MeV). One electronvolt is defined as the amount of kinetic energy gained by a single unbound electron when it accelerates through an electric potential of one Volt, thereof eV. Its value is  $e = 1.602 \times 10^{-19}\text{C}$  which is the electric charge, multiplied with one Volt, which equals  $1.602 \times 10^{-19}\text{eV}$  or  $1.602 \times 10^{-19}\text{J}$ .

$$1\text{MeV} = 10^6\text{eV} = 10^6 \cdot 1.602 \times 10^{-19}\text{J} = 1.602 \times 10^{-13}\text{J} \quad (6.3)$$

### 6.1.2 Calculating dose using LET

As explained i section 3.2.3, LET is energy deposited in a material through ionization when a particle crosses the material. LET is equal the energy loss a particle suffer by crossing a material, which means that we can use the bethe bloch formula that is expressed in equation 3.1. By looking at the total LET for a IC, we are able to calculate our way to the dose. The energy loss of a particle is highly energy dependent, but for short distances it can be assumed to be constant without getting too much error.

Two energies was used when exposing components at OCL, The first time we had a proton beam with a energy of 28 MeV, the two other times we had a beam of 25 MeV. DUT was placed 130 cm from beam exit, which means that the protons will suffer some energy loss in the air between beam-exit and DUT. To make the work easier for us, a energy loss calculator program [23] was used to calculate the *energy loss* for a 28 MeV and a 25 MeV proton beam in air, we get respectively  $17.516 \frac{\text{MeVcm}^2}{\text{g}}$  and  $19.201 \frac{\text{MeVcm}^2}{\text{g}}$ . By multiplying with the density of air which is

$\rho_{air} = 0.001275 \frac{\text{g}}{\text{cm}^3}$ , we get  $22.3 \frac{\text{keV}}{\text{cm}}$  and  $24.5 \frac{\text{keV}}{\text{cm}}$ . This means that the energy of the protons when they collide into DUT are:

$$E_{proton1} = 28 - (130\text{cm} \times 22.3 \frac{\text{keV}}{\text{cm}}) \approx 25\text{MeV} \quad (6.4)$$

$$E_{proton2} = 25 - (130\text{cm} \times 24.5 \frac{\text{keV}}{\text{cm}}) \approx 22\text{MeV} \quad (6.5)$$

By using the same energy loss calculator we get that the energy loss in silicon (which a IC mostly consist of), are:

$$-\frac{dE}{dx}(25\text{MeV}) = 17.1 \frac{\text{MeV}\text{cm}^2}{\text{g}} \quad (6.6)$$

$$-\frac{dE}{dx}(22\text{MeV}) = 18.9 \frac{\text{MeV}\text{cm}^2}{\text{g}} \quad (6.7)$$

If we look at a single proton entering a silicon material, the energy deposited by that single proton can be expressed as,

$$\Delta E_{proton} = -\frac{dE}{dx} \cdot \Delta x \cdot \rho_{Si} \quad (6.8)$$

where  $\Delta x$  is the length segment a proton particle penetrates into the material, and  $\rho_{Si}$  is the density of silicon.

$$\rho_{Si} = 2.33 \frac{\text{g}}{\text{cm}^3} \quad (6.9)$$

To get the total energy deposited in the IC, we have to multiply the energy of a single proton with the fluence and the area of the IC. Fluence is the total flux over a given time, expressed in  $[\frac{n}{\text{cm}^2}]$ . The total energy is then:

$$\Delta E_{total} = \Delta E_{proton} \cdot \Phi \cdot A_{Si} = -\frac{dE}{dx} \cdot \Delta x \cdot \rho_{Si} \cdot fluence \cdot A_{Si} \quad (6.10)$$

Now we know the total energy depleted in a IC, which is exposed to a proton beam, and can start calculating the dose. Dose is energy per mass, as said in section 6.1.1. That means that the absorbed Dose in silicon can be expressed as,

$$Dose(Si) = \frac{-\frac{dE}{dx} \cdot \Delta x \cdot \rho_{Si} \cdot \Phi \cdot A}{m_{Si}} \quad (6.11)$$

where  $m_{Si}$  is the mass of silicon.

$m_{Si}$  can be expressed in terms of silicon density, see equation 6.9, multiplied with the volume ( $V_{Si}$ ), which is Area ( $A_{Si}$ ) times thickness ( $d_{Si}$ ). Assuming that the protons enters the silicon in a straight line, the path segment  $\Delta x$  is equal the thickness, which then gives us,

$$Dose(Si) = \frac{-\frac{dE}{dx} \cdot \Delta x \cdot \rho_{Si} \cdot \Phi \cdot A}{\rho_{Si} \cdot A_{Si} \cdot d_{Si}} = -\frac{dE}{dx} \cdot fluence = \left[ \frac{MeV}{g} \right] \quad (6.12)$$

To get the dose in Rad instead of  $\frac{MeV}{g}$ , we have to multiply with the converting factor given in equation 6.3 and divide on the factor given in equation 6.2, this gives us:

$$Dose[Rad(Si)] = \frac{1.602 \cdot 10^{-13} \cdot -\frac{dE}{dx} \cdot fluence}{10^{-5}} = 1.602 \cdot 10^{-8} \cdot -\frac{dE}{dx} \cdot fluence \quad (6.13)$$

### 6.1.3 Calculating dose using FLUKA simulations

The program FLUKA can be used to simulate particles with a user given energy in whatever material you want. We simulated a proton beam with energy of 28 MeV and 25 MeV in air, and set our DUT-position 130 cm away from beam exit. The results can be seen in table 6.1.

As said in the introduction to this chapter, the known values after a radiation test are, exposed time, scintillator counts, current consumption, output data of the DUT and cross section from the SRAM detector.

The procedure to calculate the dose are first to find the proton fluence. This is found by first converting from scintillator counts to SEU, by multiplying with

Energy at beam exit	28 MeV	25 MeV
Dose/primary particle at DUT[Gy]	4.08E-10	2.94E-10
Primary particles at Beam exit	1	1
Primary particles at DUT	0.1331	8.57E-2
Beam intensity reduction at DUT	7.51	11.67

Table 6.1: FLUKA simulation with 28MeV proton beam

converting factor, and divide on the cross section. The converting factor was found as explained in section 5.1.3 and the results can be found in appendix A.1. The cross section is a known value. Fluence can then be found as seen in equation 6.14 and the flux as in equation 6.15.

$$Fluence_{DUT} = \frac{SEU}{CS} \quad (6.14)$$

$$Flux = \frac{Fluence}{time} \quad (6.15)$$

Now we can take use of the FLUKA simulation results. The simulation results tells us how many protons will hit DUT when one proton will be sent out from the beam exit, and what dose this will give the DUT. By using the calculated Fluence for DUT, found in equation 6.14, we can find the fluence at beam exit by dividing on *primary particles at DUT* from the simulation results, see equation 6.16. Then we can use *dose per primary particle at DUT* from the result and multiply with the Fluence at beam exit, which gives us the dose in gray for the DUT, see equation 6.17. By multiplying with 100 we get the dose in Rad.

$$Fluence_{BE} = \frac{fluence_{DUT}}{primary_{particlesDUT}} \quad (6.16)$$

$$Dose_{DUT}[Gy] = Fluence_{BE} \times \frac{Dose}{primary_{particleatDUT}} \quad (6.17)$$

#### 6.1.4 Comparison of LET and FLUKA

To compare LET calculations with FLuka simulation we need an example. If we look at the test result for radiation of MAX3748:

time	2472
proton energy Beam exit	25 MeV
scintillator counts	3109238
scintillator counts to SEU SRAM	0.473
Cross section	1.14E-6

Table 6.2: Results after radiation of MAX3748

Both of the methods to calculate dose requires the fluence. The fluence is given by scintillator counts, conversion value from scintillator counts to SEU on SRAM, and cross section, see equation 6.14. For MAX3748 the fluence is

$$Fluence_{MAX3748} = \frac{3109238 \cdot 0.473}{1.14 \cdot 10^{-6}} = 1.29 \cdot 10^{12} \quad (6.18)$$

### Calculations using LET

To calculate the dose using LET, just follow the steps as given in section 6.1.2. We start by calculating the energy when entering the integrated circuit 130 cm away from beam exit. This is found in equation 6.4 to be 22 MeV. LET or energy loss for a 22 MeV proton particle in silicon, is calculated in equation 6.5 to be 17.1 MeV.

Fluence is found in equation 6.18. By using equation 6.13 we get the total dose in Rad to be:

$$Dose[Rad(Si)] = 1.602 \cdot 10^{-8} \cdot 17.1 \cdot 1.29 \cdot 10^{-2} = 353.4kRad \quad (6.19)$$

### Calculations using FLUKA simulations

Calculating using FLUKA simulation is a easy process. First calculate Fluence at Beam exit, from equation 6.16. And use that value to calculate the dose as seen in equation 6.17.

$$Fluence_{BE} = \frac{1.29 \cdot 10^{12}}{0.0857} = 1.51 \cdot 10^{13} \quad (6.20)$$

$$DoseDUT[Gy] = 1.51 \cdot 10^{13} \cdot 2.94 \cdot 10^{-10} = 4425.4Gy = 442.54kRad \quad (6.21)$$

## Discussion

We can see that the FLUKA results give 20 % higher dose than with calculation using LET. That means for lower doses, the deviation will be much smaller. For example for ADN2814, the calculated does using LET is 85.6 kRad and simulation results gives us 107.1 kRad.

when calculating LET for a given IC we calculated with constant energy drop through the air before colliding with the IC and through the IC. In reality energy loss will increase as the energy decreases, this means that the calculated dose is a little smaller than the actual dose.

When it comes to FLUKA simulation, we don't really have control of what is calculated and which values are used. But the program is used for advance simulations for people at CERN and all over the world, and is a acknowledged program.

Which of these calculations gives us the most reliable calculation, can be discussed. There are a small error from approximation using LET. But then again, since we know about these approximations, we know that the energy should be a little higher than the calculated value. And can be sure that the calculated dose is at least not higher than the actual dose. From the FLUKA simulations we don't really know how the program calculates, it may be very accurate or it could do approximations as well. Data given to the program from the user, can also be incorrect and cause some error, even though this is not likely to happen.

There may also be other sources of errors, like that the proton beam given at the lab (it may differ from 25 MeV which it is said to be), and the conversion factor found in the beam setup. Nevertheless, the dose calculations doesn't need to be totally accurate, we only need to know the dose level, and then both of the methods are good enough. The dose values used further in this work are from FLUKA simulation, that is because this method was easiest to use.

## 6.2 Results from OCL

### 6.2.1 Calibration process

As explained in chapter 5.1.3, we had to start by finding the center of the beam. The laser was first placed in a position pointing a what thought to be center. Then we placed a film in front of the beam exit and DUT area. By seeing how the film

looked like after irradiated, we got a felling of where the center was. A example of two films from the beam exit and DUT area can be seen in figure 6.2.1.

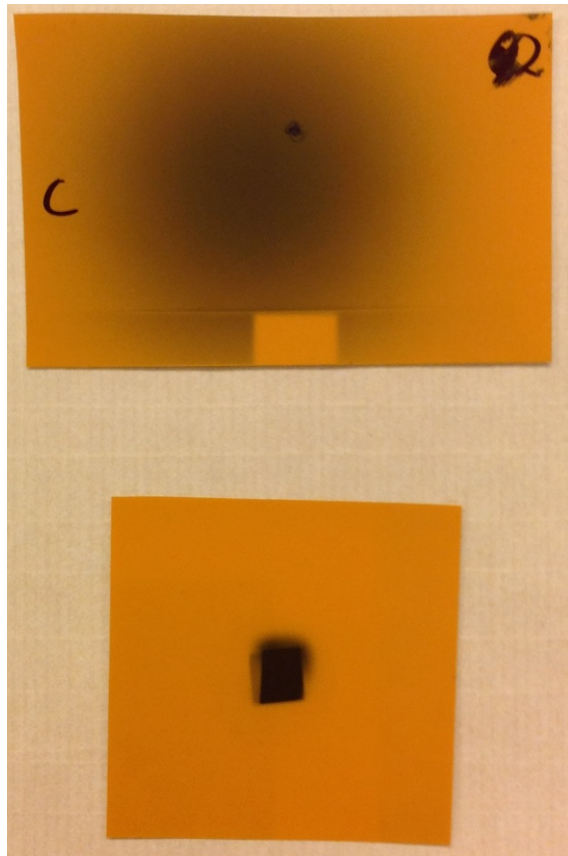


Figure 6.2.1: Example of radiation films after radiation, DUT area (top) and bream exit (button). Where the laser where pointing is marked with a dot.

Now we had a feeling of where center is compared to where the laser was pointing. The SRAM detector was placed with one of the SRAM chips at where the laser was pointing. This position was called position zero  $(x,y) = (0,0)$ . From irradiated films, we knew approximately how much we had to move to be in center of the beam. In table 6.3 you can see the results from our calibration 15.11.2013. You can see that position  $x = -2,5$  cm and  $y = -1$  cm gives highest relation between SEU and scintillator counts. A total of 4 tests in that position was done and the average value gives us 0,0948. Beam setup data from all other days at OCL can be found in appendix A. When we irradiated the different PCBs, we didn't have SEU data, but we had scintillator counts, the relation value was used to convert from scintillator counts to SEU. We wanted to have the SEU value, because the cross section for a SEU on the SRAM detector is known. The cross section is the probability that an incoming particle will induce an SEU, and the value can be found in equation 6.22. From cross section we can calculated the fluence of the beam.

$$CS = 1,14e - 6 \quad (6.22)$$

Calibration test nr.:	x	y	Scint rel	SEU(SRAM)	SEU(SRAM)/sc
1	-0,8	-1	27798	1463	5,26E-02
2	-1,3	-1	17721	1239	6,99E-02
3	-1,8	-1	12904	1203	9,32E-02
4	-2,3	-1	13361	1276	9,55E-02
5	-2,8	-1	12786	1238	9,68E-02
6	-3,3	-1	12342	1156	9,37E-02
7	-2,5	-1	11696	1223	1,05E-01
8	-2,5	-1,5	11027	1075	9,75E-02
9	-2,5	-2	11835	1063	8,98E-02
10	-2,5	-0,5	15593	1540	9,88E-02
11	-2,5	0	12620	1034	8,19E-02
12	-2,5	-1	65280	5999	9,19E-02
13	-2,5	-1	52752	4803	9,10E-02
14	-2,5	-1	57229	5250	9,17E-02

Table 6.3: Calibration tests 15.11.2013

### 6.2.2 Test results

In this section the result from radiation irradiation at OCL will be presented and discussed. Every IC will be presented for them self. In table 6.4 and 6.5 you can see how long each ICs has been exposed to radiation, the dose they have been received and if an error occurred.

Device	Exposed time[s]	Dose[Rad]	Error
<i>TPS51200</i>	2065	41800	No
<i>MIC69302WU<sub>1</sub></i>	2240	164000	No
<i>SN74AVCB164245<sub>1</sub></i>	967	65200	No
<i>SN74AVC2T245<sub>1</sub></i>	860	4600	Yes
<i>QS3VH257<sub>1</sub></i>	795	52800	No
<i>SY89831<sub>1</sub></i>	1251	93500	No

Table 6.4: Tests at OCL 15.nov 2013

Device	Exposed time[s]	Dose[Rad]	
<i>ADN2814/run1</i>	1273	20200	Yes
<i>ADN2814/run2</i>	2286	324900	Yes
<i>MAX3748</i>	2384	442200	No
<i>TPS51200<sub>2</sub></i>	-*	-*	-*
<i>MIC69302WU<sub>2</sub></i>	1385	383800	No
<i>SN74AVCB164245<sub>2</sub></i>	526	201400	No
<i>SN74AVC2T245<sub>2</sub></i>	478	161600	No
<i>QS3VH257<sub>2</sub></i>	264	110300	No
<i>SY89831U<sub>2</sub></i>	921	165800	No

\* The board wouldn't work at test time

Table 6.5: Tests at OCL 27-28.nov 2013

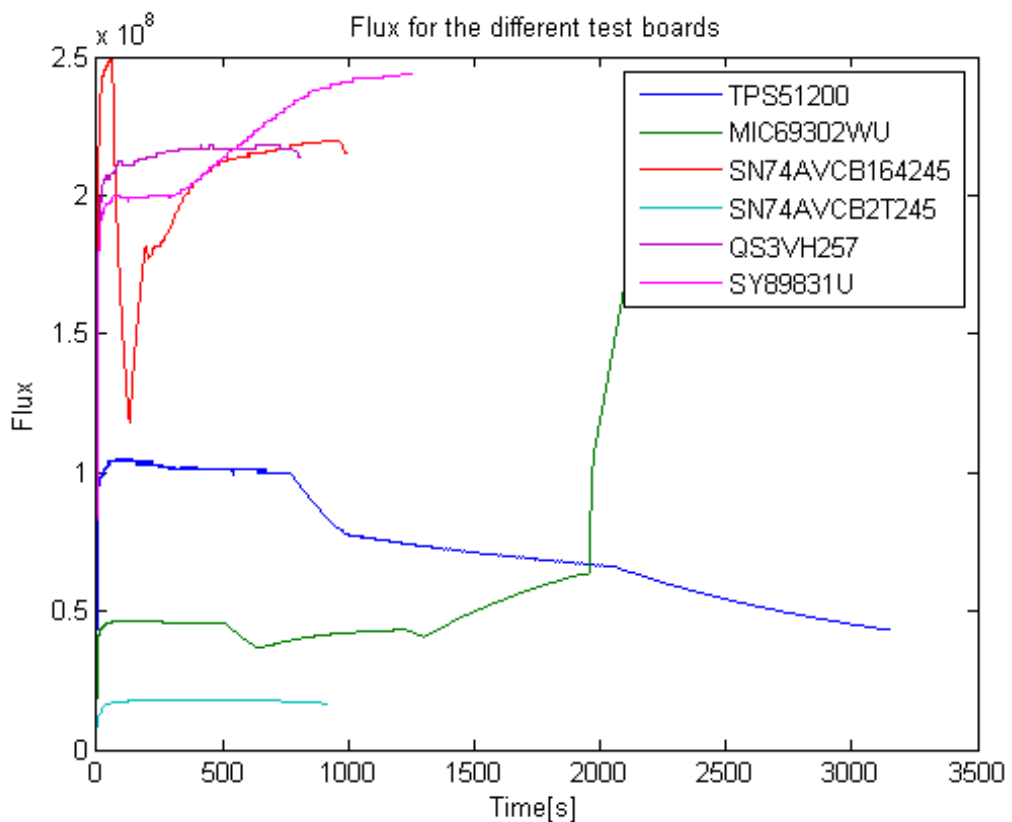


Figure 6.2.2: flux for each component radiated 15.11.2013

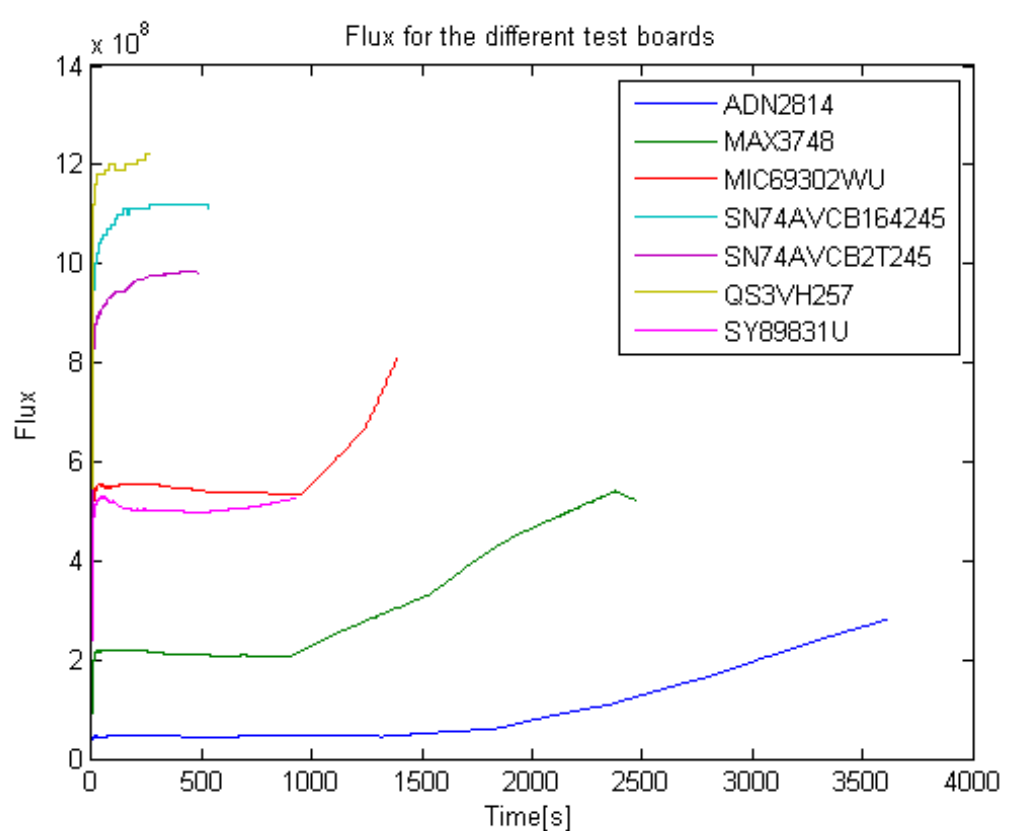


Figure 6.2.3: flux for each component radiated 15.11.2013

In figure 6.2.2 and 6.2.3 you can see graphs of flux vs time for the different test boards. The reason the graphs don't go as linear as one would expect, is that the beam sometimes stopped and had to restarted, and that we increased and decreased the intensities as we wanted.

### 6.2.3 TPS51200

This was the first board that was tested. The intensity was a little low on this test. To make the testing process faster the intensity was increased during the later experiments.

The IC worked after a dose of 40kRad, but we could see a little increase in current after a dose of 25 kRad. The output voltage is close to stable, a few mV up and down, but not noteworthy. Two PCBs of this type was tested, but only one worked when we was at OCL to do the testing.

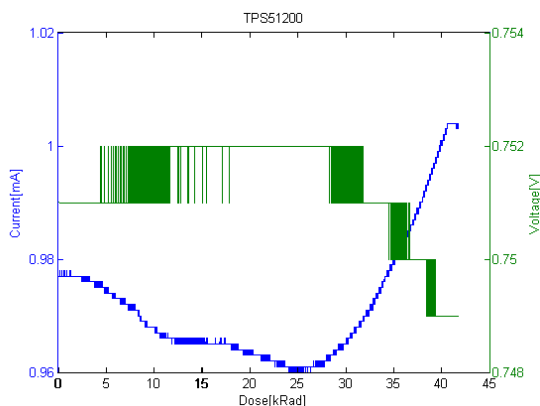


Figure 6.2.4: TPS51200 - Current/Voltage vs Dose

### 6.2.4 MIC69302WU

The first board was tested 15.11.13 and the second board was tested 28.11.13. During the test of the first board we increased the intensity of the beam quite allot, that can be seen from the flux graph, in figure 6.2.2.

This IC had an unexpected reaction to irradiation. You can see from both of the graphs that the current is decreasing and voltage is increasing, normally we would expect the opposite, or at least that the current would increase. As seen from the graph in figure 6.2.5 it starts quite early to decrease in current, but as you can see it also stabilize after a while. The output voltage is mostly stable, there were a increase of 2% on both of the tests.

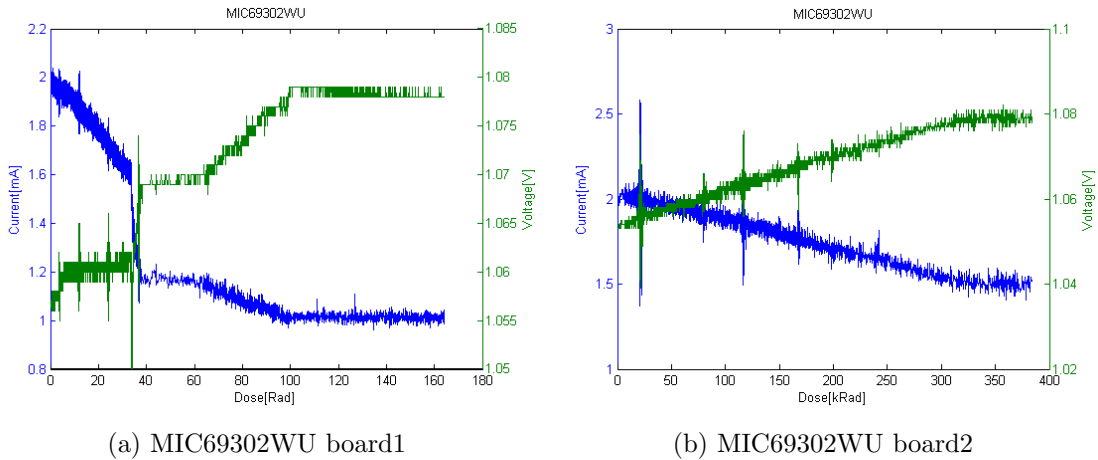


Figure 6.2.5: MIC69302WU - Current/Voltage vs Dose

### 6.2.5 SN74AVCB164245

It can be seen that the characteristics on the two test board are different, the reason for this is maybe because of different output load. The reason for the “jumps” in current is because the output is constantly changing from on to off, with a gap of 4 seconds. This chips is not effected by radiation before a dose of approx 40kRad. That is more than enough for the purposes we are going to use this for.

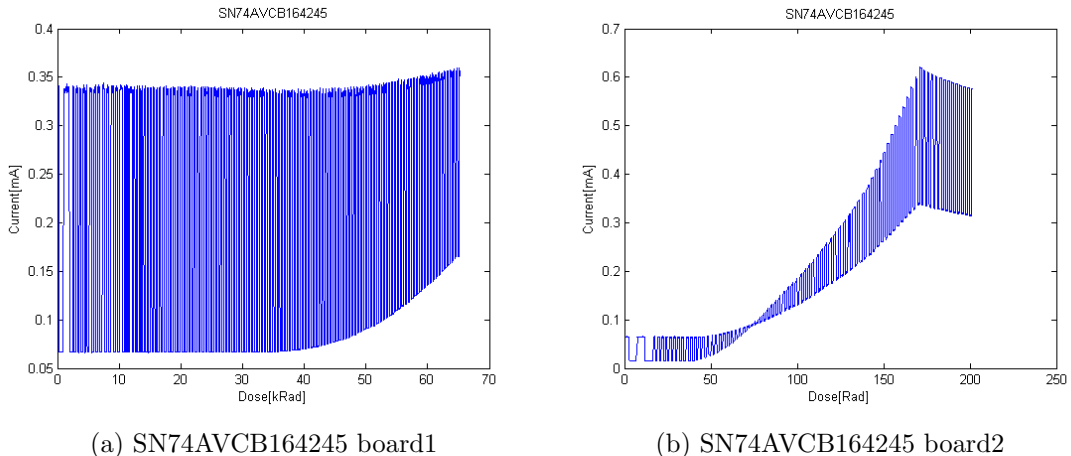


Figure 6.2.6: SN74AVC2T245 - Current vs Dose

### 6.2.6 SN74AVC2T245

Something went wrong on the first test. After 740 s and a dose of 98 Rad the chips output was stuck at 1. The reason for this is unknown, I fear that this might be defected before we started the test, since it gives a totally different characteristics than test board nr 2. The input was switching from high to low every 4 second. If

we look at the test results from board 2, the current goes unchanged up to 40 kRad, and that is more than enough.

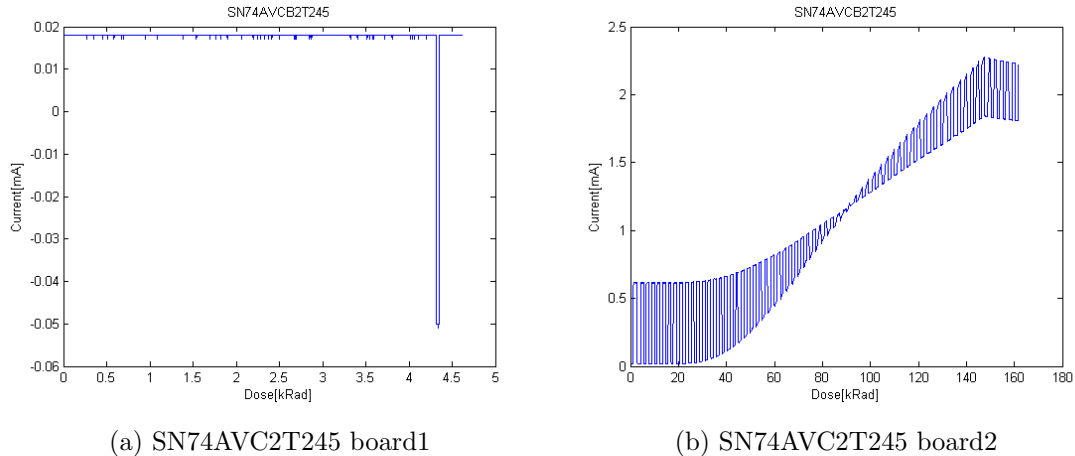


Figure 6.2.7: SN74AVC2T245 - Current vs Dose

### 6.2.7 QS3VH257

The select input was changed every 4 second and the inputs(I0A, I0B, I0C, I0D, I1A, I1B, I1C and I1D) was inverted every 18 second.

The two test boards worked fine through the tests. We see that we have small increase in current before 30 kRad, after that it increases quite allot. We couldn't see any errors on the output during the experiment, but it should probably not be exposed to more than 30 kRad.

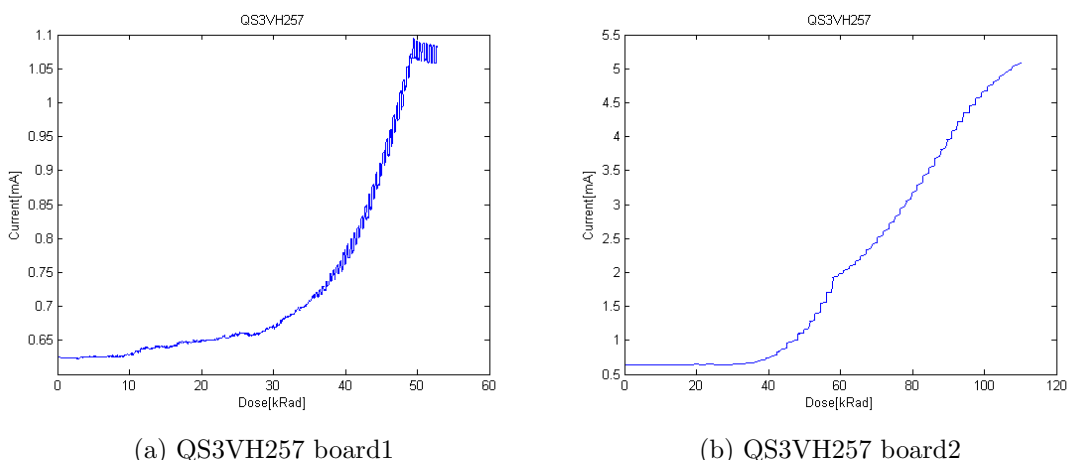


Figure 6.2.8: QS3VH257 - Current vs Dose

### 6.2.8 SY89831

This IC required a high current to work, and since the labVIEW DAQ device only delivers 5mA on the analog outputs, a combination of the modified MIC69302WU as described in section 4.1.2 and the 5V output on the DAQ was used. This gave us a output of 3.3 V and a current limit of 200 mA. Here a  $20\Omega$  resistor was used to measure current instead of a  $220\Omega$  resistor, this was to reduce the voltage drop over the resistor because of the high current consumption.

A difference in characteristics can also be seen here. This may be because two different footprint for the PCB was used, and therefore some difference can be seen. We see a small increase in current on both of the boards, but not noteworthy, compared to how much current this IC is using.

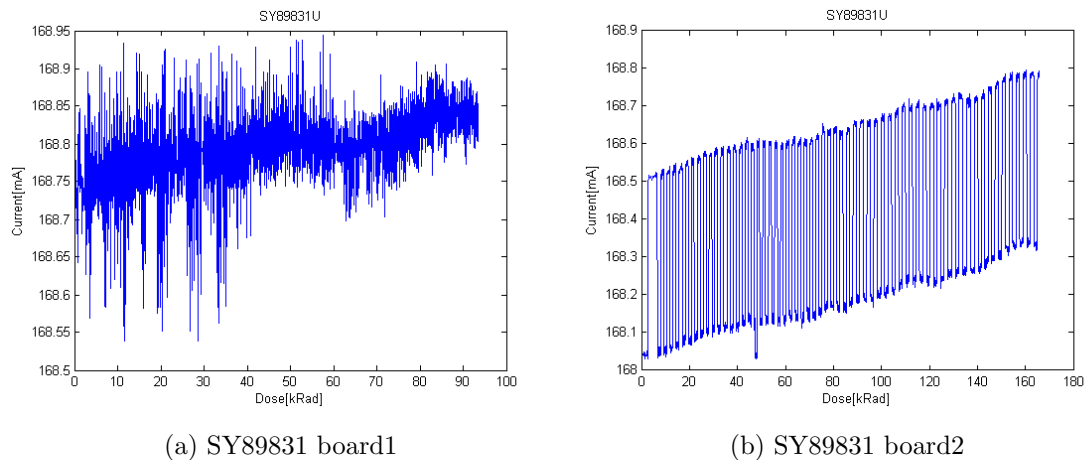


Figure 6.2.9: SY89831 - Current vs Dose

### 6.2.9 ADN2814

This IC is a little special and was hard to get a good test on. This is a clock and data return circuit, with a limiting amplifier. The SF2 board was used to code a clock and data into a differential Manchester signal, that was sent into the IC. Out of the IC we get a LVDS clock and LVDS Manchester signal. The Manchester coded data signal was decoded on SF2 board, so that we get out a clock and data. The data was tested by delaying the original data through a few D-latches, so that the original and returned data was close to synced. Then we could compare the original data with the one from the IC through a XOR-function. This function was triggered by a 80 Mhz clock from the SF2 board. If they aren't equal when the clock rises, a 1 will be added to a counter. The value of the counter was constantly sent through the UART of the SF2 board.

The way the clock was tested was a little harder process since the clock was so fast

(160 Mhz). This was solved, was by adding a third clock with the same frequency (160 Mhz) that was  $90^\circ$  of from the two others, when this goes high I called on the XOR-function, to see if the two other clocks are the same. if they are alike, nothing happens, if they are not the program adds 1 to a counter, which constantly writes its current value to a Universal Asynchronous Receiver/Transmitter (UART). The problem here is that for each time the SF2 board was programmed the clock was slightly different, that made either the clock out of sync or the data out of sync, so the code didn't always work as it should. This circuit also requires allot of current, therefore the same solution as for SY89831 was used, using MIC69302WU as a power supply and measure the current on that PCB.

The current didn't change before a dose of 200 kRad had been received, but we got a clock error at a dose of  $\sim 11$  kRad, and a data error after a dose of  $\sim 8$  kRad. How good this test really is, could be discussed, since we don't have any data on the clock and data, other than that the XOR-function failed. What really failed, and how much is impossible to know. It could be a slightly delay on a clock or the data, or maybe the clock just disappeared for a moment.

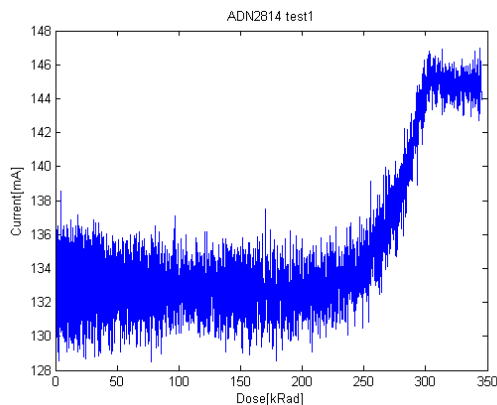


Figure 6.2.10: ADN2814 - Current vs Dose

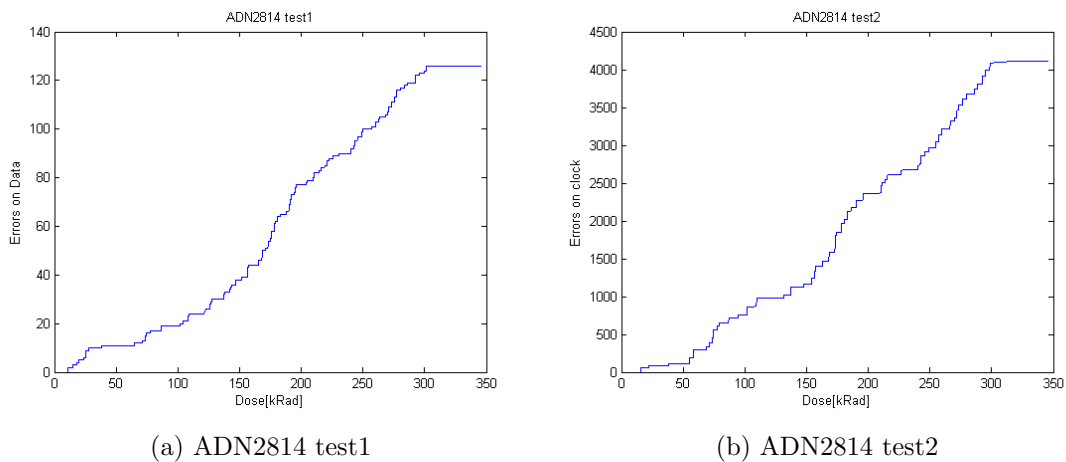


Figure 6.2.11: ADN2814 - Relative errors vs Dose

### 6.2.10 MAX3748

This circuit has the same purpose as ADN2814, the difference is that this one only return the limited Manchester coded signal, and no clock. The process for testing the data is the same as for the ADN2814. The decoding process return clock and data, but since they are related to another, a error on the clock would mean an error at the data. So by measuring data, we can be sure that there are no clock errors as well.

After a dose of over 400 kRad this chip still worked, and current consumption was stable through the hole irradiation process.

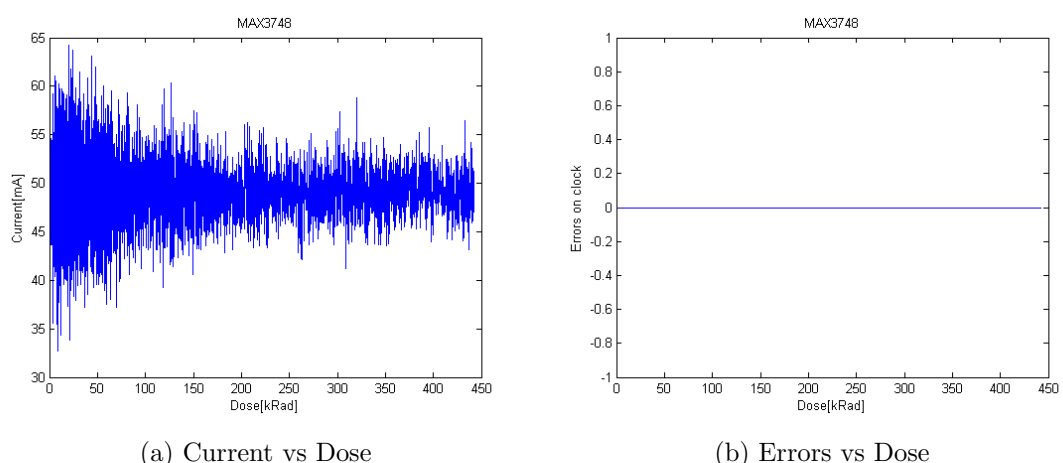


Figure 6.2.12: MAX3748

## 6.3 Discussion of the result

Most of the testing was done 15.nov and 28.nov. The other days was used to get familiar with the instruments and equipment that was being used, to prepare the setup and setting up the beam. There are almost impossible to get the same beam two days at a row. Each day of testing is therefore different from each other. Since the testing was conducted in two periods and a total of 4 test days, there are allot of uncertainties regarding the beam. And that is also why we had to do calibration each day at start-up.

When we were going to measure the intensity at the beam exit, we placed a Faraday cup in front of the beam, and connected it to a amperemeter on the control panel, but since the current is so small, the measuring instrument will be affected by air currents, and there are also allot of uncertainties in the instruments. Therefore we only used the Faraday cup and the amperemeter, to get a rough estimate of the actual intensity.

The are also some uncertainties regarding the DAQ device form NI. When measuring digital signal, we don't know if it goes from 0 V to 3.3 V as we would expect. Maybe in reality the low voltage is actually 0.4 V and high voltage is actually 2.8 V. If this is the case, it could be a problem with using this in our design.

As said before in 5.1.3, if a component survives 10 times more than what it will receive in a period of 10 years in ALICE, that is 1-2 kRad, than it can be used in the design of RCU2. Having that in mind, I would say that every component tested would have a green flag even though we had some errors when testing SN74AVC2T245 and ADN2814. Since the result after testing board two of SN74AVC2T245 was positive we can assume that something was wrong with the first board. When it comes to ADN2814, it would be nice to have more time in the lab to test this even more, since the test done gave us so unclear results. If a better test would be made, I'm sure that this would perform much better.

# **Chapter 7**

## **Conclusion**

# Appendix A

## Some Appendix

### A.1 Beam setup data

Calibration test nr.:	x	y	Scint rel	SEU(SRAM)	SEU(SRAM)/sc
1	0	0	23813	1971	8,28E-02
2	0	-0,5	37930	3867	1,02E-01
3	0	-1	27527	2817	1,02E-01
4	0	-1,5	34413	3360	9,76E-02
5	0	-2	32713	2763	8,45E-02
6	0,5	0	38753	2709	6,99E-02
7	-0,5	0	23420	2483	1,06E-01
8	-1	0	20611	2232	1,08E-01
9	-1,5	0	21014	2410	1,15E-01
10	-1,5	0	20676	2260	1,09E-01
11	-2	0	35787	3776	1,06E-01
12	-2,5	0	27847	2512	9,02E-02

Table A.1: Calibration tests 14.11.2013

Calibration test nr.:	x	y	Scint rel	SEU(SRAM)	SEU(SRAM)/ sc
1	-0,8	-1	27798	1463	5,26E-02
2	-1,3	-1	17721	1239	6,99E-02
3	-1,8	-1	12904	1203	9,32E-02
4	-2,3	-1	13361	1276	9,55E-02
5	-2,8	-1	12786	1238	9,68E-02
6	-3,3	-1	12342	1156	9,37E-02
7	-2,5	-1	11696	1223	1,05E-01
8	-2,5	-1,5	11027	1075	9,75E-02
9	-2,5	-2	11835	1063	8,98E-02
10	-2,5	-0,5	15593	1540	9,88E-02
11	-2,5	0	12620	1034	8,19E-02
12	-2,5	-1	65280	5999	9,19E-02
13	-2,5	-1	52752	4803	9,10E-02
14	-2,5	-1	57229	5250	9,17E-02

Table A.2: Calibration tests 15.11.2013

# Bibliography

- [1] K. Aamodt, A. A. Quintana, R. Achenbach, S. Acounis, D. Adamova, C. Adler, and the rest of the ALICE Collaboration, “The alice experiment at the cern lhc,” *JOURNAL OF INSTRUMENTATION*, vol. 3, AUG 2008.
- [2] K. Safarik, “Overview of recent alice results,” *Nuclear Physics A*, vol. 904, pp. 27C–34C, May 2013.
- [3] CERN, “Cern accelerators.” <http://cds.cern.ch/record/42384>.
- [4] F. Faccio, “Alice information site.” <http://aliceinfo.cern.ch/>.
- [5] K. Roeed, *Single Event Upsets in SRAM FPGA based readout electronics for the Time Projection Chamber in the ALICE experiment*. PhD thesis, University of Bergen, Norway, 2009.
- [6] microsemi, “Smartfusion2 product brief,” 2014. [http://www.microsemi.com/document-portal/doc\\_download/132721-smartfusion2-product-brief](http://www.microsemi.com/document-portal/doc_download/132721-smartfusion2-product-brief).
- [7] T. F. Thorsteinsen, *Kompendium i Straalingsfysikk - FYS231/233*. Bergen: University of Bergen, 1995.
- [8] D. M. H. Neil H. E. Weste, *CMOS VLSI Design - A Circuit and System Perspective*. Addison-Wesley, 4 edition ed., 2011.
- [9] G. F. Knoll, *Radiation Detector and Measurement*. John Wiley and Sons, 3 edition ed., 2000.
- [10] R. Baumann, “Radiation-induced soft errors in advanced semiconductor technologies,” *Device and Materials Reliability, IEEE Transactions on*, vol. 5, pp. 305–316, Sept 2005.
- [11] V. Balashov, *Interaction of particles and Radiation with Matter*. Springer-Verlag, 1997.
- [12] F. Faccio, “Radiation effects in the electronics for cms.” [http://lhcb-elec.web.cern.ch/lhcb-elec/papers/radiation\\_tutorial.pdf](http://lhcb-elec.web.cern.ch/lhcb-elec/papers/radiation_tutorial.pdf).
- [13] F. M. T.R Oldham, “Total ionizing dose effects in mos oxides and devices,” *IEEE TRANSACTIONS ON NUCLEAR SCIENCE*, 2003.

- [14] T. Granlund and N. Olsson, “A comparative study between proton and neutron induced seu in srams,” 2006.
- [15] G. K. Tsiledakis, *Scale Dependence of Mean Transverse Momentum Fluctuations at Top SPS Energy measured by the CERES experiment and studies of gas properties for the ALICE experiment*. PhD thesis. Darmstadt: Technische Universitat Darmstadt, 2006.
- [16] B. H. Straume, “Straalingstester og utvikling av bestraalingsposedyre for alice tpc-elektronikken,” Master’s thesis, University of Bergen, Norway, 2006.
- [17] K. Roeed, “Irradiation tests of altera sram-based fpgas,” Master’s thesis, University of Bergen, Norway, 2004.
- [18] A. Velure, “Design, implementation and testing of sram based neutron detectors,” Master’s thesis, University of Bergen, Norway, 20011.
- [19] N. I. Corporation, “User guide and specifications ni usb-6008/6009,” April 2014. <http://www.ni.com/pdf/manuals/371303m.pdf>.
- [20] T. Instruments, “Tps51200 - sink/source ddr termination regulator,” February 2008. <http://www.ti.com/lit/ds/slus812/slus812.pdf>.
- [21] M. Berg, “Field programmable gate array (fpga) single event effect (see) radiation testing,” February 2012.
- [22] U. University, “Information about tsl,” April 2014. [http://www.ts1.uu.se/About\\_TSL/](http://www.ts1.uu.se/About_TSL/).
- [23] S. Meroli, “Energy loss calculator,” 2014. <http://meroli.web.cern.ch/meroli/EnergyLossCalculation.html>.